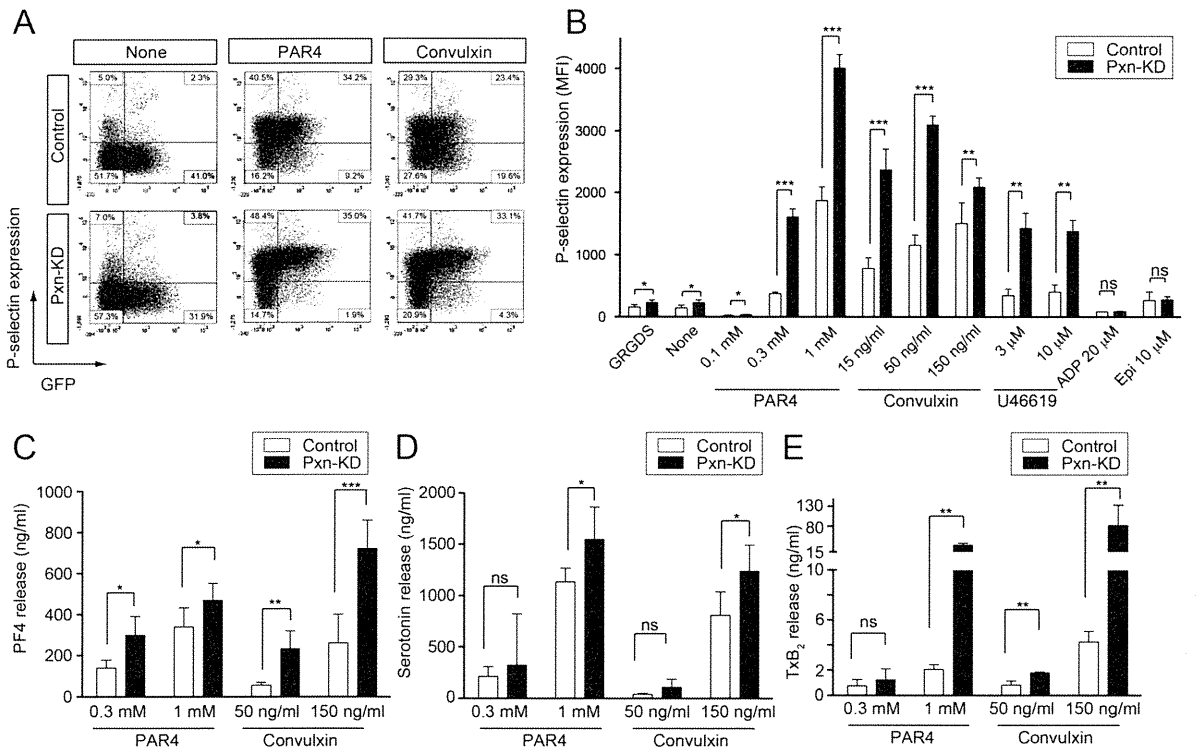

Figure 3 The release reaction is enhanced in Pxn-KD platelets. Bone marrow cells transduced with LentiLox-sh-control-GPIbα (Control) or LentiLox-sh-paxillin-GPIbα (Pxn-KD) at an MOI of 5 were transplanted into lethally irradiated recipient mice. **(A)** P-selectin expression on GFP-positive platelets stimulated with or without 1 mmol/L AYPGKF or 50 ng/mL convulxin was assessed by flow cytometry. The plots represent the degree of GFP expression (horizontal) and P-selectin expression (vertical). **(B)** Columns and error bars represent the mean ± s.d. of P-selectin expression after stimulation in GFP-positive platelets ($n = 3$–5). (C–E) Washed platelets were stimulated with the indicated agonist for 15 min, and then the concentrations of PF4 **(C)**, serotonin **(D)**, and TxB_2 **(E)** were measured in the supernatants. Columns and error bars represent the mean ± s.d. ($n = 5$). Open bars: control platelets; black bars: Pxn-KD platelets. Statistical significance was determined using Student's *t*-test. $^*P < 0.05$, $^{**}P < 0.01$, and $^{***}P < 0.001$ vs. control.

secondary effects of platelet aggregation, influx of extracellular calcium, and release reactions, we preincubated the platelets with EDTA, apyrase, and SQ29548. Intracellular calcium mobilization induced by the GPVI agonist convulxin and G protein-coupled receptor stimulation with AYPGKF was rather decreased by Pxn-KD (Figure 5B). These data suggest that paxillin targets downstream signaling of calcium mobilization or a calcium-independent signaling pathway.

To explore the importance of calcium-independent signaling pathways in Pxn-KD platelets, we employed BAPTA-AM, an intracellular calcium chelator, to exclude the effect of calcium mobilization. Because JON/A requires extracellular calcium for antibody binding, we assessed P-selectin expression induced by an agonist. Pretreatment with BAPTA-AM significantly suppressed P-selectin expression in both control and Pxn-KD platelets (Figure 5C). On the other hand, P-selectin expression elicited by an agonist was still observed in Pxn-KD platelets even in the presence of BAPTA-AM (Figure 5C). These data indicate that downstream signaling from intracellular calcium mobilization is amplified by Pxn-KD, and the calcium-independent pathway is activated by Pxn-KD to increase platelet activation.

Pxn-KD augments platelet adhesion and thrombus formation in vivo

Finally, we examined the contribution of paxillin to thrombus formation in vivo. To visualize thrombus formation in vivo, we used a direct visual technique based on confocal microscopy in mesenteric capillaries [26]. Thrombus formation in this system was initiated by the production of ROS following laser irradiation [26]. Laser irradiation-induced thrombus formation was significantly enhanced in Pxn-KD platelets (Figure 6A and 6B and Additional files 6 and 7). In addition, there was an enhancement of thrombus formation initiated by $FeCl_3$ in large femoral arteries (Additional file 8). Moreover, bleeding times after tail clipping significantly shortened in Pxn-KD experiments (Figure 6C). These findings support

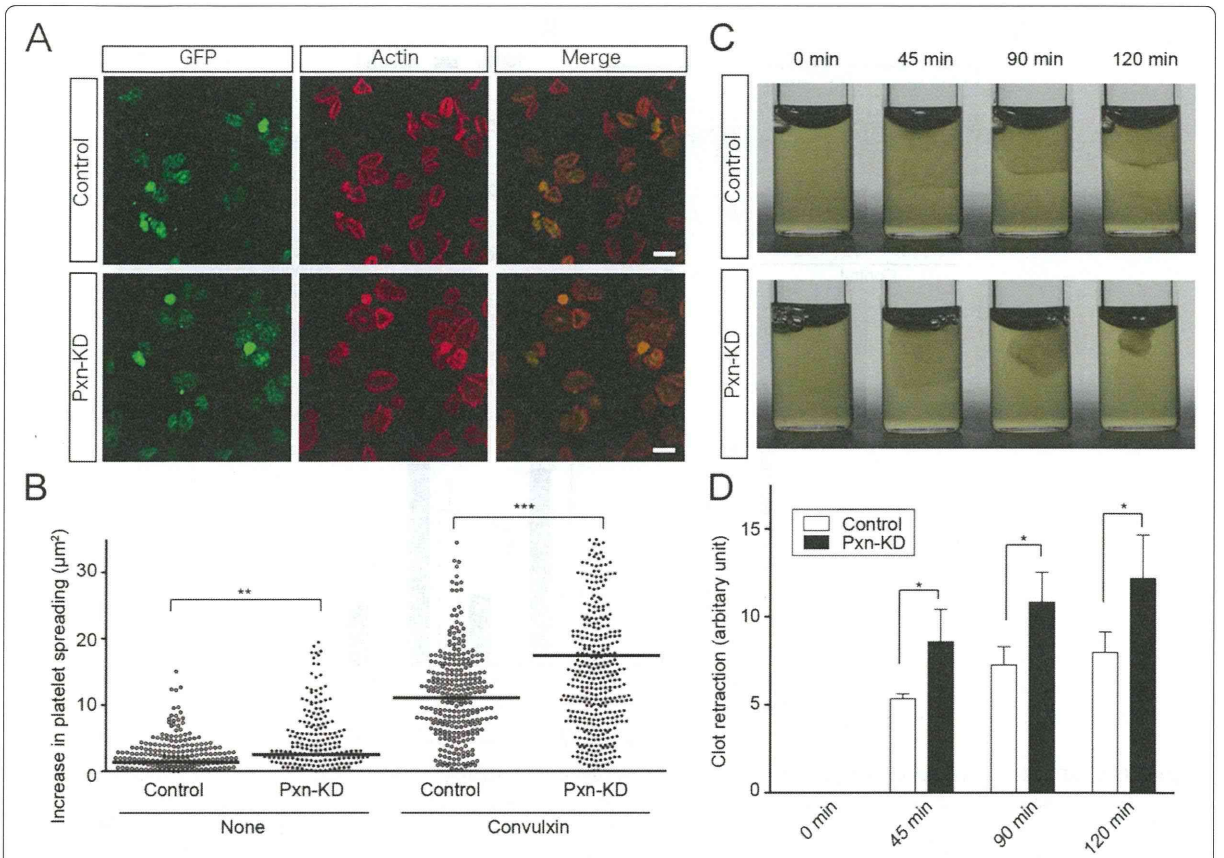

Figure 4 Pxn-KD platelets exhibit augmented outside-in signaling. (A) Control and Pxn-KD platelets treated with 50 ng/mL convulxin were allowed to adhere on immobilized fibrinogen for 30 min. The platelets were then fixed and stained with an anti-GFP antibody (green; left panel) and rhodamine-conjugated phalloidin (red; middle panel). The merged images show colocalization of GFP and actin staining (yellow; right panel). Original magnification, ×600; Bar, 5 μm. Data are representative of three independent experiments. **(B)** Platelets treated with or without 50 ng/mL convulxin were incubated in dishes coated with 400 μg/mL fibrinogen for 30 min. The area of cell spreading was quantified by ImageJ software. The mean platelet size on BSA was subtracted from the total spread area on fibrinogen to determine the actual increase in platelet spreading. The horizontal bar denotes the mean, and each symbol denotes an individual cell ($n = 281–394$ cells). **(C)** Clot retraction of platelet-rich plasma consisting of diluted human plasma and control or Pxn-KD platelets was initiated by 0.1 U/mL thrombin and then photographed at 0, 45, 90, and 120 min. **(D)** Clot retraction was quantified by measuring serum formation extruded by clot retraction. Columns and error bars represent the mean ± s.d. ($n = 3$). Open bars: control platelets; black bars: Pxn-KD platelets. Statistical significance was determined using Student's *t*-test. $^{*}P < 0.05$, $^{**}P < 0.01$, and $^{***}P < 0.001$ vs. control.

our hypothesis that paxillin is an important negative regulator of platelet activation and thrombus formation in vivo.

Discussion

Here, we found that the LIM protein paxillin is a negative regulator of platelet activation in mice. The negative regulation of platelet activation by paxillin was not limited to a specific signaling pathway, because Pxn-KD enhanced platelet activation in response to a variety of agonists. We also confirmed that thrombus formation was augmented in Pxn-KD platelets in vivo. This finding is notable because several previous reports suggest that changes in paxillin function actually reduce integrin signaling [13,14]. Furthermore, a previous finding in platelets has demonstrated the possible role of paxillin as a negative feedback regulator after integrin ligation to regulate the activity of Lyn tyrosine kinase [17]. However, this mode of regulation cannot fully explain the phenotypes of Pxn-KD platelets, because both outside-in and inside-out signaling were augmented by Pxn-KD. Our results reveal a new cellular function of paxillin and indicate new mechanisms that modulate platelet activation.

The most interesting result of this study was that Pxn-KD significantly enhanced the upstream signaling pathways that converge on platelet activation. Appropriate inhibition of the platelet response is essential to control pathological thrombus formation. It is well known that the mediators that enhance intracellular cAMP or cGMP

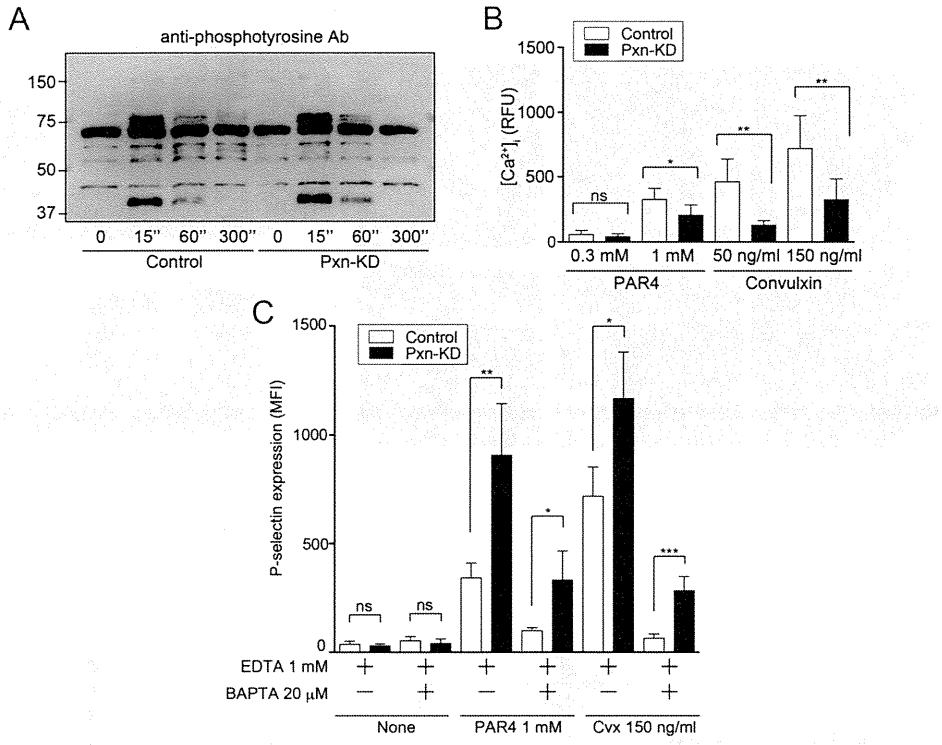

Figure 5 Pxn-KD fails to increase tyrosine phosphorylation and calcium mobilization. (A) Washed platelets obtained from control and Pxn-KD experiments were stimulated with 150 ng/mL convulxin for the indicated times. The cell lysates were resolved by SDS-polyacrylamide gel electrophoresis and then immunoblotted with an anti-phosphotyrosine mAb (4G10). The data shown are representative of three independent experiments. **(B)** Control and Pxn-KD platelets were labeled with GFP-Certified™ FluoForte™ dye. Changes in intracellular calcium levels after stimulation with an indicated concentration of AYPGKF or convulxin were then measured every 30 s. Data are expressed as the relative fluorescence unit (RFU) measured using a microplate spectrofluorometer (excitation, 530 nm; emission, 570 nm). The peak calcium concentration was measured after stimulation (open bars: control platelets; black bars: Pxn-KD platelets). Columns and error bars represent the mean ± s.d. (n = 5–8). Statistical significance was determined by the Student's t-test. **(C)** Control and Pxn-KD platelets were pretreated with 1 mmol/L EDTA and/or 20 μmol/L BAPTA-AM for 10 min, and then stimulated with or without 1 mmol/L AYPGKF or 150 ng/mL convulxin. P-selectin expression on GFP-positive platelets was determined by flow cytometry. Columns and error bars represent the mean ± s.d. of P-selectin expression (n = 4).

levels, including prostacyclin, prostaglandin E_1, and nitric oxide, are strong extrinsic inhibitors of platelet activation [27]. These extrinsic mediators ameliorate the broad platelet activation elicited by various agonists [27]. Intrinsic negative regulators of platelet activation have been identified recently, but many of these proteins only control a specific receptor signaling pathway. GPVI-mediated immunoreceptor tyrosine-based activation motif (ITAM) signaling is regulated by immunotyrosine-based inhibitory motif (ITIM)-containing receptors including platelet endothelial cell adhesion molecule 1 and carcinoembryonic antigen-related cell adhesion molecule 1 [28,29]. Furthermore, Lyn tyrosine kinase has been reported to inhibit ITAM signaling by inducing tyrosine phosphorylation of ITIM [28]. It has also been reported that binding of a regulator of G-protein signaling to the Giα subunit limits platelet responsiveness to the receptor, which is independent of Rap1b [30]. Conversely, paxillin may downregulate platelet activity by modulating a common pathway, because Pxn-KD resulted in marked platelet hyperactivation in response to stimulation of tyrosine phosphorylation-based receptors and G protein-coupled receptors.

Although paxillin is reportedly involved in various integrin-mediated cellular functions, many of these functions are limited to outside-in signaling pathways. Paxillin-deficient embryos show embryonic lethality, and the phenotype closely resembles that of fibronectin-deficient mice [31]. Moreover, paxillin-deficient fibroblasts show reductions in cell migration and tyrosine phosphorylation following cell adhesion [31]. Chimeric integrin αIIbβ3 with a cytoplasmic tail substitution of α4β1 or α9β1, which facilitates paxillin binding, significantly inhibits cell spreading, but does not affect αIIbβ3-dependent cell adhesion [18,19]. Inhibition of paxillin binding to integrin α4 inhibits leukocyte recruitment to an inflammatory site [32]. These data suggest important roles of paxillin in outside-in signaling by direct interaction with the integrin α-subunit. However, in this study, inside-out and outside-

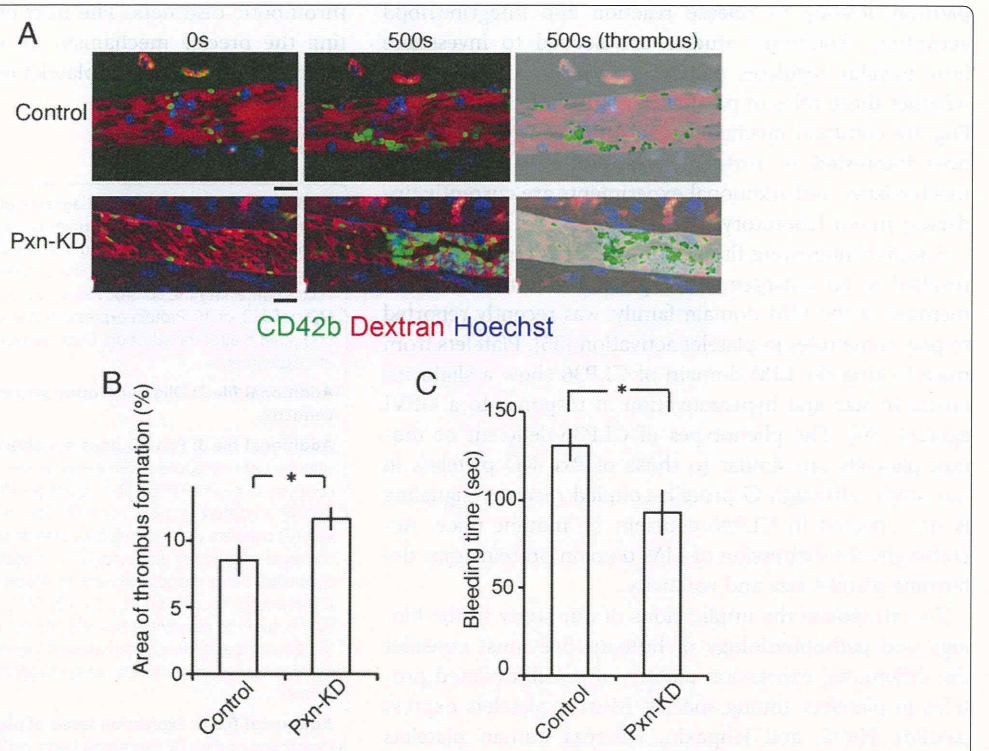

Figure 6 Pxn-KD in platelets expedites thrombus formation in vivo. (A) Intravital imaging of thrombus formation by laser irradiation of mesenteric arterioles in mice with control or Pxn-KD platelets. Thrombus formation was increased in mice with Pxn-KD platelets following laser irradiation. Bar, 10 μm. The right panel shows the results of quantification of the thrombus area. **(B)** Percentage areas of thrombus within blood vessels after laser irradiation. Columns and error bars represent the mean ± s.e.m. ($n = 40$ vessels in five mice/group). **(C)** Tail bleeding times were assessed as described in the Methods. Columns and error bars represent the mean ± s.e.m. (n = four mice/group). Statistical significance was determined using Student's *t*-test. $^*P < 0.05$ vs. control.

in signaling of integrin αIIbβ3 were increased in Pxn-KD platelets, even though paxillin failed to interact with platelet-specific integrin αIIb [19]. It is possible that other signaling pathways in platelets are modulated by paxillin, which is independent of direct interactions with integrins.

An issue that remains unresolved is the precise mechanism governing the negative regulatory function of paxillin in platelet activation. As described above, Rathore et al. previously reported that integrin αIIbβ3-dependent platelet aggregation induced tyrosine phosphorylation of paxillin and Hic-5 in platelets, leading to the binding of Csk, which controls activation of the Src family of tyrosine kinases [17]. Csk preferentially binds to paxillin in murine platelets that coexpress paxillin and Hic-5 [17]. Furthermore, the interaction abolishes the activity of Lyn, but not Fyn or Src. It is possible that paxillin acts as a negative feedback regulator of outside-in signaling by modulating Lyn activity after ligand binding to integrin αIIbβ3 [17]. However, this mechanism does not fully explain the functional roles of paxillin in platelets. Our data suggest that paxillin controls additional proximal signaling pathways for platelet activation. Pxn-KD did not directly augment the conformational changes of integrin αIIbβ3 expressed on Chinese hamster ovary cells (Additional file 9), tyrosine phosphorylation, or calcium mobilization induced by phosphoinositide turnover. These data suggest that paxillin negatively controls downstream signaling of calcium mobilization or a calcium-independent signaling pathway. In addition, calcium mobilization was rather reduced by Pxn-KD. It is therefore possible that negative feedback exists to prevent further activation of Pxn-KD platelets, or phosphoinositide turnover is directly modulated by Pxn-KD.

Our data suggest that several mechanisms may increase platelet activation by Pxn-KD. Notably, calcium-independent actions by Pxn-KD appear to exist, because P-selectin expression elicited by an agonist was still observed in Pxn-KD platelets even in the presence of BAPTA-AM. A previous report has suggested that coordinated signaling through both $G_{12/13}$ and G_i causes integrin αIIbβ3 activation, despite a small increase in intracellular calcium [33]. In addition, $G_{12/13}$ and G_i signaling activates integrin αIIbβ3 in Gq-deficient mice [34]. It is possible that paxillin modify the calcium-independent signaling

pathway leading to release reaction and integrinαIIbβ3 activation. Additional studies are needed to investigate how paxillin regulates platelet activation, and to assess whether these roles of paxillin in control of cellular signaling are common mechanisms in other cell types. We are now interested in further investigation of the precise mechanisms, and additional experiments are currently underway in our laboratory.

Another interesting finding of our study is that Pxn-KD resulted in an enlargement of platelet volume. CLP36, a member of the LIM domain family, was recently reported to play some roles in platelet activation [35]. Platelets from mice lacking the LIM domain of CLP36 show a slight increase in size and hyperactivation in response to a GPVI agonist [35]. The phenotypes of CLP36-deficient or mutant platelets are similar to those of Pxn-KD platelets in our study, although G protein-coupled receptor signaling is not affected in CLP36-deficient or mutant mice. Accordingly, the expression of LIM domain proteins may determine platelet size and reactivity.

To extrapolate the implications of our study to the biology and pathophysiology of humans, we must consider the differential expression pattern of paxillin-related proteins in platelets among species. Murine platelets express paxillin, Hic-5, and leupaxin, whereas human platelets only express Hic-5 [17]. Hagmann et al. reported that a switch from paxillin to Hic-5 expression should occur during the late phase of megakaryopoiesis in humans [15]. A recent report has described platelet functions in Hic-5-deficient mice [36]. Hic-5-deficient mice exhibit prolonged bleeding times, and the loss of Hic-5 in platelets slightly impairs integrin αIIbβ3 activation induced by thrombin, but not other agonists including convulxin, U46619, and ADP [36]. Although the hemostatic defect in Hic-5-deficient mice, as assessed by tail bleeding, is not fully explained by a mild defect in platelet function, it is possible that the structurally related proteins paxillin and Hic-5 play opposing roles in the regulation of platelet function in murine platelets. Leupaxin, another LIM protein that is predominantly expressed in leukocytes, has been reported to play an inhibitory role in B cell receptor signaling [37], which is similar to the role of paxillin reported in this study. In human platelets, which only express Hic-5, it will be necessary to elucidate whether Hic-5 acts as a positive regulator of integrin αIIbβ3 activation.

In summary, we have shown that paxillin is a negative regulator of platelet activation in mouse platelets. Modulation of platelet activation by Pxn-KD may originate in the augmentation of common signaling pathways, leading to integrin αIIbβ3 activation, release reactions, and Tx biosynthesis. Modulation of the LIM protein function might be an attractive candidate therapeutic target capable of strongly suppressing unexpected platelet activation in thrombotic disorders. The next challenge will be elucidating the precise mechanism by which paxillin regulates the signaling pathway in platelet activation.

Additional files

Additional file 1: Schematic diagrams of the lentiviral vector used in this study. (A) Schematic diagram of the lentiviral vector. (B) Locations of the oligonucleotides encoding the shRNAs in the mouse *paxillin* (*Pxn*) gene. (C) Mouse embryonic fibroblasts were transduced with a lentiviral vector containing the control, Pxn-1, Pxn-2, or Pxn-3 shRNA sequences at MOIs of 1, 3, or 10. Protein expression was determined by immunoblotting at 48 h after transduction. Data are representative of three independent experiments.

Additional file 2: Oligonucleotide sequences of siRNA cloned into LentiLox.

Additional file 3: Pxn-KD does not affect granule contents. Bone marrow cells transduced with LentiLox-sh-control-GPIbα (Control) or LentiLox-sh-paxillin-GPIbα (Pxn-KD) at an MOI of 5 were transplanted into lethally irradiated recipient mice. (A) The morphology of control and Pxn-KD platelets was examined by transmission electron microscopy, and the areas of granules and cytoplasm in each platelet were independently quantified using ImageJ software for Macintosh. Columns and error bars represent the mean ± s.d. ($n = 53–70$). (B–C) Washed platelets were lysed to measure the concentrations of platelet factor 4 (PF4) (B) and serotonin (C). Columns and error bars represent the mean ± s.d. ($n = 4$). Statistical significance was determined using Student's t test. $^{***}P < 0.001$ vs. control.

Additional file 4: Expression levels of platelet-specific glycoproteins. Description of data: (A) Expression levels of GPIIb/IIIa (integrin αIIbβ3) (left panel), GPIb (middle panel), and GPVI (right panel) in control (dark gray) and paxillin-knockdown platelets (light gray). (B) Columns and error bars represent the mean ± s.d. of the mean fluorescence intensity (MFI) of antibody binding ($n = 5$). Statistical significance was determined using Student's t test. $^{*}P < 0.05$, $^{**}P < 0.01$, and $^{***}P < 0.001$ vs. control.

Additional file 5: Effects of apyrase and SQ29548 on agonist-induced integrin αIIbβ3 activation and P-selectin expression in control and Pxn-KD platelets. Platelets pretreated without or with 5 U/mL apyrase and 10 μmol/L SQ29548 were stimulated with the indicated agonists. JON/A binding (A) and P-selectin expression (B) on GFP-positive platelets were assessed by flow cytometry. Column and error bars represent the mean ± s.d. of the mean fluorescence intensity (MFI) ($n = 3–4$). Statistical significance was determined using Student's t test. $^{*}P < 0.05$, $^{**}P < 0.01$, and $^{***}P < 0.001$ vs. control.

Additional file 6: Intravital imaging of thrombus formation by laser irradiation of mesenteric arterioles in mouse with control platelets.

Additional file 7: Intravital imaging of thrombus formation by laser irradiation of mesenteric arterioles in mice with Pxn-KD platelets.

Additional file 8: Thrombus formation in femoral arteries induced by FeCl3. (A) Intravital imaging of thrombus formation 5 mins after FeCl3 treatment in femoral arteries in mice with control or paxillin knock-down platelets (Pxn-KD). The black arrows indicate the direction of blood flow, and triangles show the developed thrombus. Bar, 100 μm. (B) Areas of thrombus within arteries 20 mins after laser irradiation. Columns and error bars represent the mean ± s.e.m. (n = 8 arteries in four mice/group).

Additional file 9: Knock-down of paxillin does not affect talin-dependent activation of integrin αIIbβ3 in CHO cells. (A) Schematic representation of the lentiviral vectors used in this experiment. (B–D) αIIbβ3-CHO cells were transduced with lentiviral vectors expressing a control shRNA sequence and GFP (Control), the paxillin shRNA sequence and GFP (Pxn-KD), a control shRNA sequence and the GFP-Talin FERM domain (Control-FERM), or the paxillin shRNA sequence and the GFP-Talin FERM domain (Pxn-KD-FERM). (B) Lysates obtained from the transduced cells were immunoblotted with anti-GFP polyclonal antibody, anti-paxillin monoclonal antibody, and anti-vinculin monoclonal antibody. (C) PAC-1 binding after transduction in the presence or absence of 1 mmol/L GRGDS was assessed by

flow cytometry. Data are representative of four independent experiments. (D) Columns and error bars represent the mean ± s.d. of PAC-1 binding (n = 4). Statistical significance was determined using Student's *t* test.

Abbreviations

Pxn-KD: Paxillin-knockdown; Tx: Thromboxane; shRNA: Short hairpin RNA; GRGDS: Gly-Arg-Gly-Asp-Ser; ROS: Reactive oxygen species; ITAM: Immunoreceptor tyrosine-based activation motif; ITIM: Immunotyrosine-based inhibitory motif.

Competing interests

The authors declare that they have no competing interests.

Authors' contributions

Contribution: AS, TO, and SN designed the study, performed the experiments, analyzed the data, and wrote the manuscript; HS performed the experiments and wrote the manuscript; SM, JM, KK, and YS analyzed the data and revised the manuscript. All authors read and approved the final manuscript.

Acknowledgements

We would like to thank Tamaki Aoki, Naoko Ito and Masanori Ito (Jichi Medical University) for providing excellent technical assistance. This study was supported by Grants-in-Aid for Scientific Research (T.O., S.M., J.M.), the Funding Program for Next Generation World-Leading Researchers (S.N.), the Translational Systems Biology and Medicine Initiative from JST (S.N.), the Support Program for Strategic Research Infrastructure from the Japanese Ministry of Education and Science (Y.S.), and Health, Labour and Science Research Grants for Research on HIV/AIDS and Research on Intractable Diseases from the Japanese Ministry of Health, Labour and Welfare (Y.S.).

Author details

[1]Research Division of Cell and Molecular Medicine, Center for Molecular Medicine, Jichi Medical University School of Medicine, 3111-1 Yakushiji, Shimotsuke, Tochigi 329-0498, Japan. [2]Division of Cardiovascular Medicine, Department of Internal Medicine, Jichi Medical University School of Medicine, 3111-1 Yakushiji, Shimotsuke, Tochigi 329-0498, Japan. [3]Department of Cardiovascular Medicine, The University of Tokyo, 7-3-1 Hongo, Bunkyo, Tokyo 113-8655, Japan. [4]Translational Systems Biology and Medicine Initiative, The University of Tokyo, 7-3-1 Hongo, Bunkyo, Tokyo 113-8655, Japan. [5]Department of Morphological and Biomolecular Research, Nippon Medical School, 1-1-5 Sendagi, Bunkyo, Tokyo 113-8602, Japan.

Received: 26 November 2013 Accepted: 9 December 2013
Published: 2 January 2014

References

1. Coller BS: **Historical perspective and future directions in platelet research.** *J Thromb Haemost* 2011, **9**(Suppl 1):374–395.
2. Watson SP, Auger JM, McCarty OJ, Pearce AC: **GPVI and integrin alphaIIb beta3 signaling in platelets.** *J Thromb Haemost* 2005, **3**:1752–1762.
3. Varga-Szabo D, Pleines I, Nieswandt B: **Cell adhesion mechanisms in platelets.** *Arterioscler Thromb Vasc Biol* 2008, **28**:403–412.
4. Shattil SJ, Kim C, Ginsberg MH: **The final steps of integrin activation: the end game.** *Nat Rev Mol Cell Biol* 2010, **11**:288–300.
5. Siess W: **Molecular mechanisms of platelet activation.** *Physiol Rev* 1989, **69**:58–178.
6. Guidetti GF, Torti M: **The small GTPase rap1b: a bidirectional regulator of platelet adhesion receptors.** *J Signal Transduct* 2012, **2012**:412089.
7. Moser M, Legate KR, Zent R, Fassler R: **The tail of integrins, talin, and kindlins.** *Science* 2009, **324**:895–899.
8. Moser M, Nieswandt B, Ussar S, Pozgajova M, Fassler R: **Kindlin-3 is essential for integrin activation and platelet aggregation.** *Nat Med* 2008, **14**:325–330.
9. Nieswandt B, Moser M, Pleines I, Varga-Szabo D, Monkley S, Critchley D, Fassler R: **Loss of talin1 in platelets abrogates integrin activation, platelet aggregation, and thrombus formation in vitro and in vivo.** *J Exp Med* 2007, **204**:3113–3118.
10. Petrich BG, Fogelstrand P, Partridge AW, Yousefi N, Ablooglu AJ, Shattil SJ, Ginsberg MH: **The antithrombotic potential of selective blockade of talin-dependent integrin alpha IIb beta 3 (platelet GPIIb-IIIa) activation.** *J Clin Invest* 2007, **117**:2250–2259.
11. Cantor JM, Ginsberg MH, Rose DM: **Integrin-associated proteins as potential therapeutic targets.** *Immunol Rev* 2008, **223**:236–251.
12. Glenney JR Jr, Zokas L: **Novel tyrosine kinase substrates from Rous sarcoma virus-transformed cells are present in the membrane skeleton.** *J Cell Biol* 1989, **108**:2401–2408.
13. Brown MC, Turner CE: **Paxillin: adapting to change.** *Physiol Rev* 2004, **84**:1315–1339.
14. Deakin NO, Turner CE: **Paxillin comes of age.** *J Cell Sci* 2008, **121**:2435–2444.
15. Hagmann J, Grob M, Welman A, Van Willigen G, Burger MM: **Recruitment of the LIM protein hic-5 to focal contacts of human platelets.** *J Cell Sci* 1998, **111**(Pt 15):2181–2188.
16. Osada M, Ohmori T, Yatomi Y, Satoh K, Hosogaya S, Ozaki Y: **Involvement of Hic-5 in platelet activation: integrin alphaIIbbeta3-dependent tyrosine phosphorylation and association with proline-rich tyrosine kinase 2.** *Biochem J* 2001, **355**:691–697.
17. Rathore VB, Okada M, Newman PJ, Newman DK: **Paxillin family members function as Csk-binding proteins that regulate Lyn activity in human and murine platelets.** *Biochem J* 2007, **403**:275–281.
18. Liu S, Slepak M, Ginsberg MH: **Binding of Paxillin to the alpha 9 integrin cytoplasmic domain inhibits cell spreading.** *J Biol Chem* 2001, **276**:37086–37092.
19. Liu S, Thomas SM, Woodside DG, Rose DM, Kiosses WB, Pfaff M, Ginsberg MH: **Binding of paxillin to alpha4 integrins modifies integrin-dependent biological responses.** *Nature* 1999, **402**:676–681.
20. Coller BS, Anderson K, Weisman HF: **New antiplatelet agents: platelet GPIIb/IIIa antagonists.** *Thromb Haemost* 1995, **74**:302–308.
21. Ohmori T, Kashiwakura Y, Ishiwata A, Madoiwa S, Mimuro J, Sakata Y: **Silencing of a targeted protein in in vivo platelets using a lentiviral vector delivering short hairpin RNA sequence.** *Arterioscler Thromb Vasc Biol* 2007, **27**:2266–2272.
22. Rubinson DA, Dillon CP, Kwiatkowski AV, Sievers C, Yang L, Kopinja J, Rooney DL, Ihrig MM, McManus MT, Gertler FB, *et al*: **A lentivirus-based system to functionally silence genes in primary mammalian cells, stem cells and transgenic mice by RNA interference.** *Nat Genet* 2003, **33**:401–406.
23. Ohmori T, Kashiwakura Y, Ishiwata A, Madoiwa S, Mimuro J, Furukawa Y, Sakata Y: **Vinculin is indispensable for repopulation by hematopoietic stem cells, independent of integrin function.** *J Biol Chem* 2010, **285**:31763–31773.
24. Suzuki H, Okamura Y, Ikeda Y, Takeoka S, Handa M: **Ultrastructural analysis of thrombin-induced interaction between human platelets and liposomes carrying fibrinogen gamma-chain dodecapeptide as a synthetic platelet substitute.** *Thromb Res* 2011, **128**:552–559.
25. Bergmeier W, Schulte V, Brockhoff G, Bier U, Zirngibl H, Nieswandt B: **Flow cytometric detection of activated mouse integrin alphaIIbbeta3 with a novel monoclonal antibody.** *Cytometry* 2002, **48**:80–86.
26. Nishimura S, Manabe I, Nagasaki M, Kakuta S, Iwakura Y, Takayama N, Ooehara J, Otsu M, Kamiya A, Petrich BG, *et al*: **In vivo imaging visualizes discoid platelet aggregations without endothelium disruption and implicates contribution of inflammatory cytokine and integrin signaling.** *Blood* 2012, **119**:e45–e56.
27. Smolenski A: **Novel roles of cAMP/cGMP-dependent signaling in platelets.** *J Thromb Haemost* 2012, **10**:167–176.
28. Ming Z, Hu Y, Xiang J, Polewski P, Newman PJ, Newman DK: **Lyn and PECAM-1 function as interdependent inhibitors of platelet aggregation.** *Blood* 2011, **117**:3903–3906.
29. Wong C, Liu Y, Yip J, Chand R, Wee JL, Oates L, Nieswandt B, Reheman A, Ni H, Beauchemin N, Jackson DE: **CEACAM1 negatively regulates platelet-collagen interactions and thrombus growth in vitro and in vivo.** *Blood* 2009, **113**:1818–1828.
30. Signarvic RS, Cierniewska A, Stalker TJ, Fong KP, Chatterjee MS, Hess PR, Ma P, Diamond SL, Neubig RR, Brass LF: **RGS/Gi2alpha interactions modulate platelet accumulation and thrombus formation at sites of vascular injury.** *Blood* 2010, **116**:6092–6100.
31. Hagel M, George EL, Kim A, Tamimi R, Opitz SL, Turner CE, Imamoto A, Thomas SM: **The adaptor protein paxillin is essential for normal**

development in the mouse and is a critical transducer of fibronectin signaling. *Mol Cell Biol* 2002, **22**:901–915.
32. Feral CC, Rose DM, Han J, Fox N, Silverman GJ, Kaushansky K, Ginsberg MH: **Blocking the alpha 4 integrin-paxillin interaction selectively impairs mononuclear leukocyte recruitment to an inflammatory site.** *J Clin Invest* 2006, **116**:715–723.
33. Dorsam RT, Kim S, Jin J, Kunapuli SP: **Coordinated signaling through both G12/13 and G (i) pathways is sufficient to activate GPIIb/IIIa in human platelets.** *J Biol Chem* 2002, **277**:47588–47595.
34. Nieswandt B, Schulte V, Zywietz A, Gratacap MP, Offermanns S: **Costimulation of Gi- and G12/G13-mediated signaling pathways induces integrin alpha IIbbeta 3 activation in platelets.** *J Biol Chem* 2002, **277**:39493–39498.
35. Gupta S, Braun A, Morowski M, Premsler T, Bender M, Nagy Z, Sickmann A, Hermanns HM, Bosl M, Nieswandt B: **CLP36 Is a Negative Regulator of Glycoprotein VI Signaling in Platelets.** *Circ Res* 2012, **111**:1410–1420.
36. Kim-Kaneyama JR, Miyauchi A, Lei XF, Arita S, Mino T, Takeda N, Kou K, Eto K, Yoshida T, Miyazaki T, *et al*: **Identification of Hic-5 as a novel regulatory factor for integrin alphaIIbbeta3 activation and platelet aggregation in mice.** *J Thromb Haemost* 2012, **10**:1867–1874.
37. Chew V, Lam KP: **Leupaxin negatively regulates B cell receptor signaling.** *J Biol Chem* 2007, **282**:27181–27191.

doi:10.1186/1477-9560-12-1
Cite this article as: Sakata *et al.*: Paxillin is an intrinsic negative regulator of platelet activation in mice. *Thrombosis Journal* 2014 **12**:1.

血栓止血誌 24(6) : 588～592, 2013

◆特集：血管内皮，血管機能のイメージング解析◆

生体分子イメージングによる血栓形成・血管機能の可視化

Visualization of thrombus formation *in vivo*

西村　智 *1,2
Satoshi NISHIMURA *1,2

◇要旨◇

生体でもっとも小さく核を有さない血小板は，一方で，多彩な生理作用を持つ．しかし，従来の手法では，単一血小板は生体内で可視化することができず，生体での機能にも不明な点が多かった．我々は，一光子共焦点・二光子レーザー顕微鏡を用いた「生体分子イメージング手法」を独自に開発し，血栓症をはじめとする生活習慣病にアプローチしてきた．本手法を用いて生体内の血栓形成過程の詳細も明らかになり，iPS由来の人工血小板の機能解析も可能となっている．生体内の血小板機能を生体外で再構築し解析することも可能になっている．生体内での血小板の活性化機構と血栓止血機能，さらに多彩な生命生理現象との関わりに対して，新規アプローチを中心に紹介する．

Key words: *in vivo* imaging, thrombus, platelet, inflammation

1．はじめに　生体イメージングとは

現在，マウスからヒトにいたるまで全遺伝子が同定されたにもかかわらず，生体機能の多くは依然として不明であり，遺伝子・細胞治療，再生医療の実用化にも多くの障壁がある．その原因として，多くの研究者が，試験管内で生ずる事象と生体の間には，大きな乖離があることを感じている．

従来の医学・生物学において，多くの実験アプローチは，細胞レベル（*in vitro*）・個体レベル（*in vivo*）のそれぞれが独立した実験系により評価されている．細胞レベルでは主に培養細胞を用いた単一種の細胞が用いられ網羅的な解析がなされているが，しかし，「比較的正常に近い機能破綻」である血栓症を含む生活習慣病などの病態下では，単一細胞・単一遺伝子の異常から個体全体の異常を説明することはできない．さらに，遺伝子機能の評価に際しては，個体レベルではノックアウトマウスをはじめとした遺伝子改変動物を用いた検討がしばしば行われているものの，複雑なフィードバック機構により支配されているため，得られた表現型がどのような細胞間相互作用・組織間相互作用によってもたらされるかは不明であり，生体での真の機能解析には不十分であった．このように，生理学的状態・病態の理解には，両者（個体と細胞）を結びつける解析技術の開発が必須である．そこで，我々は独自に開発した生体分子イメージングを中心に，組織再構築の過程，免疫・炎症性細胞の動態，血栓形成メカニズムなど，多くの生命現象にアプローチしてきた．細胞間相互作用を解析することにより，今までに *in vitro* で得られた分子生物学的知見と個体の表現型の情報

*1 東京大学医学系研究科循環器内科〔〒113-0853 東京都文京区本郷 7-3-1〕
Department of Cardiovascular Medicine, The University of Tokyo
*2 東京大学システム疾患生命科学による先端医療技術開発拠点特任准教授
Translational Systems Biology and Medicine Initiative, The University of Tokyo
〔7-3-1, Hongo, Bunkyo-ku, Tokyo 123-0853, Japan〕
Tel: 03-3815-5411　Fax: 03-3814-0021　e-mail: snishi-tky@umin.ac.jp

を結びつけることが可能になると考えている．

我々は，独自に開発した「生体分子イメージング手法」を，まず，肥満した脂肪組織に適応し，メタボリックシンドロームの病態にアプローチを行ってきた．本稿では，我々の生体イメージングより明らかになった，血栓形成過程についての知見を紹介したい．

2．生体内の組織の可視化 生体分子イメージングの開発

動脈硬化のように血管が主な傷害の場になる病態だけでなく，血栓症，腫瘍やメタボリックシンドロームにおいても，血流や血管機能といった生体内のダイナミックな変化，組織学的変化に先行する初期の炎症性変化を捉えることが可能な生体内分子イメージング技術は非常に有用である．従来の生体内観察では，透過光による観察が容易な腸間膜の微小循環を用いた研究が主に行われてきたが，近年の光学観察系・蛍光プローブの開発により，蛍光物質をトレーサーとして，透過光観察が不可能な厚みを有する脂肪組織をはじめとする実質臓器の血流観察も可能となった時間・空間解像度も飛躍的に改善し，細胞内小器官レベルでの解析が可能となっている．また後述の通り高速マルチカラー二光子生体イメージングも簡便に行われるようになっている．

本邦の死因の上位を占める脳・心血管疾患の多くは血管の動脈硬化性変化を基盤とした血栓性疾患（アテローム血栓症）であると理解されている．アテローム血栓症は慢性炎症を背景とした動脈硬化巣の形成と，引き続いて起こる，動脈硬化巣の粥腫（＝アテローム）の破綻がその本態であると考えられている．破綻部位では，血小板は活性化され，血小板血栓が形成され，引き続く血液凝固系の活性化により病態が進行する．一連の過程には血小板だけでなく，各種炎症性細胞（マクロファージ・リンパ球）や血管内皮細胞とその障害，局所の血流動態が関わっている．このような多細胞からなる複雑病変とそのダイナミクスが病態の本質であるが，今まで生体内で検討する手法は存在しなかった．我々は以前より代謝異常における慢性炎症の関わりを明らかにするために，生体内における細胞動態，細胞間ネットワークの破綻を可視化手法により検討してきた．その過程で，生体内での単一血小板レベルでの血栓形成過程を世界にさきがけて可視化した

観察システムは我々が開発したもので，独自性が高いだけでなく，その解像度は従来のイメージング手法をはるかに凌駕している．マルチカラーイメージングでは，生体内で複数の細胞種を染め分けて同定するとともに，機能プローブを組み合わせ，形態と機能の同時観察が可能である（**図1**参照）．

我々は，レーザー傷害によるROS産生を伴う血栓形成モデルと生体イメージングを組み合わせ，血小板機能に異常を来す各種遺伝子改変動物における血栓形成過程を観察し，生体内での血小板機能との関係を明らかにした．我々のモデルでは楕円形を伴った血小板のみが血栓形成しており，一方，血管内皮の構築は保たれていた．炎症性サイトカインのノックアウトマウス，キメラマウスの解析の結果，TNF-αをはじめとする炎症性サイトカインが，ROS刺激下でのvWF因子の血管内皮表面への表出に関わっていることが明らかになった．さらに，IL-1，IL-6等の因子も血栓性を促進しており，これらの炎症性サイトカインは血管内皮に作用し，インテグリンシグナルと協同して，血栓の安定化に寄与していた．従来，炎症と血栓については多様な報告によりその関連が示唆されていたが，本解析により血栓形成過程のうち，血管内皮における炎症性サイトカインのシグナリングが血栓形成に関わっていることが示された[1]．

我々の血栓形成モデルでは，まずレーザー照射により活性酸素の産生が誘発されて血管内皮に血小板が付着する．活性酸素は血管内皮細胞に直接働き，パイエル小体中のvon Willebrand因子を，細胞膜表面上に移動させる．一方，活性酸素は血小板にも直接作用し，P-selectin，GPIIbIIIaといった機能蛋白が血小板表面に誘導される．その結果，血管内皮のvon Willebrand因子と血小板表面のGPIbが結合し，血栓が誘発される．その後，血小板はその数を増やし積み上り，血管内腔を狭小化し，血液の流速は遅くなる．最終的には，赤血球，もしくは，白血球により血管は閉塞する．

我々のモデルが特徴的なのは，血栓形成の全過程が数十秒で終わり，時間的に経過が極めて早いことと，画像が高解像度であることである．本モデルではレーザー照射後に血栓形成に寄与した血小板数を数えることによって血栓形成能を明確に定量可能である．従来の頸動脈に対する塩化鉄傷害モデルにおける血栓による閉塞時間とも強い相関を示しており，生体内の血小板機能を極めて鋭敏に反映していると考えられる．それだけでなく，従来の止血時間の計測では分からなかった，血栓形成の素過程が可視化されており，遺伝子改変の効果がどの過程に影響を及ぼしているかを明らかにすることができる．

我々は本手法を用い，Lnkというアダプター蛋白に注目して実験を進めた．Lnkは血球系幹細胞の維持に重要な蛋白であるが，巨核球・血小板にも発現しているが，その機能は不明であった．興味深いことに，Lnkの欠損した遺伝子改変動物では，流血中の末梢血小板数が野生型の5倍になるにも関わらず血栓性を示さず，むしろ止血時間が延長しており，Lnkの欠損が血小板機能に影響をもたらしていると考えた．骨髄移植を行い作成したLnkキメラマウスを用い，生体イメージングにより血栓形成過程を観察したところ，血球系でのみLnkが欠損したLnkキメラマウスではレーザー傷害により血小板は一過性に血管内皮に付着するものの，血栓は安定化せず血流に崩され，血小板血栓の発達が阻害されているさまが可視化された．すなわち，Lnkが血小板血栓の安定化に寄与していることが示された．分子生物学的機序としてはリン酸化したLnkが，C-Src，Fynと協同してインテグリンのシグナリングに関与していた．以上より，Lnkが生体内血栓の形成・安定化に寄与していることが明確に示された[2]．

さらにLnkの遺伝子変異がヒトにおいては，多血症・血小板無力症や骨髄増殖性疾患を引き起こすことも報告されている．多血症では血小板数は増加するものの，血小板機能は低下していることが多く，今回，Lnkノックアウトマウスでみられた表現型にきわめて近いと言え，Lnkの血小板機能における重要性がマウスだけでなく，ヒトにおいても示されている．

今後は，さらに様々な血小板機能に異常を来す遺伝子改変動物における血栓形成過程・血小板動態を観察することにより，「生体内の血栓形成の各過程における遺伝子・物質の関与」が明らかになると思われる．

3. iPS由来人工血小板の体内イメージング

近年の，多能性幹細胞（ES, iPS）の研究の進歩により，細胞療法を含む再生医学での広い範囲での臨床応用が期待されている．しかし，これらの幹細胞を用いた基礎研究を臨床現場に繋げるためには，*in vitro*での知見をヒトを対象とした研究に応用する前に，実際に試験管内で作成した細胞が，実際の個体（マウス及び大動物）の中でどのように機能しているか，どのように病変に働くかを明らかにすることは必須である．しかし，今までこれらiPS由来の分化誘導細胞の体内での細胞動態を検討する手法は存在しなかった．我々は，京都大学iPS細胞研究所江藤教授チームとの共同研究の結果，iPS細胞を誘導するのに必要な山中四因子の中のc-Mycの発現をコントロールすることにより，飛躍的かつ効率的に，ヒトiPS由来の人工血小板を作成する手法を確立した．我々は生体イメージングを用いて，こうして得られたヒトiPS由来血小板の体内動態の可視化を行った．観察に用いた免疫不全マウス（NOGマウス）の体内では，iPS由来人工血小板の細胞動態が捉えられた（**図2**）．iPS由来血小板がマウス体内を循環しているだけでなく，レーザー傷害により誘発された血栓形成部位においてはホスト血小板とiPS由来血小板が相互作用しながら血栓を形成するさまが観察された．つまり，「人工血小板は体内を循環し，血栓も作る」ことが証明されたわけである．このように，本イメージ手法はiPS分化誘導細胞を用いた細胞療法の臨床応用に向けて，安全性・有用性を評価する上できわめて有用性が高い手法と言える[3]．さらに，最近では，人工血小板の作成を飛躍的に改善する分子メカニズムがより明らかになりつつあり，臨床応用も近いと考えられる．

また，これらの人工血小板の機能解析を微小流路デバイスを使って，生体外で解析することも可能にした．たとえば，von Willebrand因子をコー

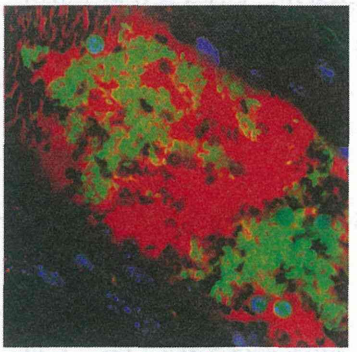

図1　生体内における血栓形成過程
レーザー照射により誘発された微小血栓の形成過程．生体イメージングとレーザー傷害を組み合わせることにより，腸間膜の毛細血管において，血栓を誘発し，血栓形成に寄与する単一血小板を可視化することが可能になった．レーザー照射により血小板血栓が発達している．

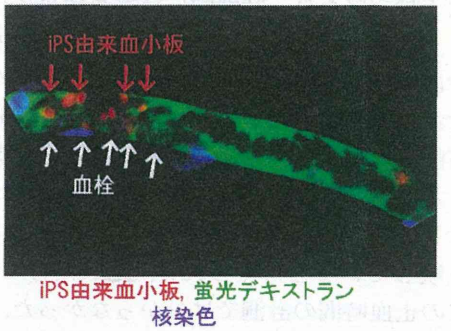

図2　生体内におけるiPS由来人工血小板の血栓形成過程
レーザー照射により誘発されたiPS由来人工血小板の血栓形成過程．
20秒のレーザー照射により人工血小板を含む血小板血栓が発達し血管径が狭小化している．

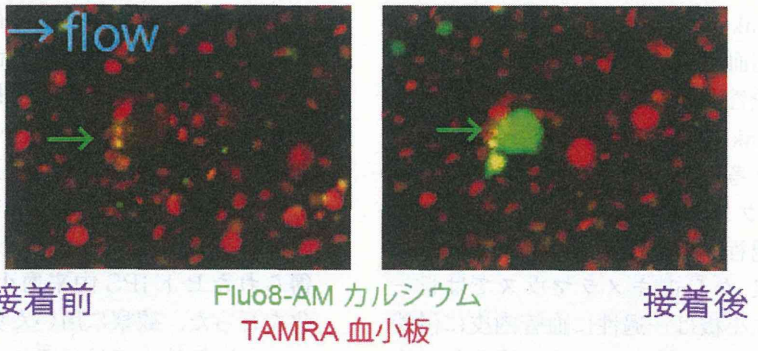

図3　微小流路デバイスによるヒトiPS細胞由来人工血小板のカルシウム応答の可視化
von Willebrand因子をコーティングしたガラス面との接着によりカルシウム上昇が接着血小板に認められる．
血小板は赤色，カルシウム応答は緑色の蛍光色素・プローブにより可視化した．

ティングしたガラススライドの上に，カルシウムインディケーターを導入した人工血小板を流し，ガラス面との接着に伴いカルシウム上昇がおきることを確認している．このように，生体内の反応を模したデバイスも開発されており，今後の展開が期待される．今後は，白血球，血管内皮，血小板の相互作用にも注目していきたい（**図3**参照）．

4. おわりに　次世代のイメージング　深部を照らす機能イメージング

我々は今まで主にニポウ式レーザー共焦点，一光子励起の組み合わせで画像取得を行ってきた．しかし，深部臓器・臓器内部の構造に関しては可視化できず，遺伝子機能も不明であった．生体の各種病態下での細胞連関・情報伝達異常をより明らかにするためには，形態と機能とを組み合わせた深部の光イメージングが今後必要になると考えられる．例えば，遺伝子改変動物を用いた遺伝子機能の光による解析を，二光子フェムト秒レーザーと高速スキャニング共焦点システムで行うというものであり，既に多くの生体内深部の知見が得られている．二光子励起による生体イメージングについては，脳組織を用いたイメージングが先行し，それ以外の臓器での知見についてはあまり研究されてこなかったのも実情である．しかし，

今後は光学機器の改良に伴う画像の改善・操作性の改善・扱いやすさ使いやすさの向上，顕微鏡システムの価格の一般化，光学プローブの開発改良，が総合的に進むと考えられ，初心者の研究者でも，これらの手法が今後可能になると考えている．

Disclosure of Conflict of Interest

The author indicated no potential conflict of interest.

文　献

1) Nishimura S, Manabe I, Nagasaki M, Kakuta S, Iwakura Y, Takayama N, Ooehara J, Otsu M, Kamiya A, Petrich B, Urano T, Kadono T, Sato S, Aiba A, Yamashita H, Sugiura S, Kadowaki T, Nakauchi H, Eto K, Nagai R：*In vivo* imaging visualizes discoid platelet aggregations without endothelium disruption and implicates contribution of inflammatory cytokine and integrin signaling. Blood **119**(8)：e45-56, 2012.
2) Nishimura S, Takizawa H, Takayama N, Oda A, Nishikii H, Morita Y, Kakinuma S, Yamazaki S, Okamura S, Tamura N, Goto S, Sawaguchi A, Manabe I, Takatsu K, Nakauchi H, Takaki S, Eto K：Lnk/Sh2b3 regulates integrin alpha-IIb-beta3 outside-in signaling in platelets leading to stabilization of developing thrombus *in vivo*. J Clin Invest **120**(1)：179-190, 2010.
3) Takayama N, Nishimura S, Nakamura S, Shimizu T, Ohnishi R, Endo H, Yamaguchi T, Otsu M, Nishimura K, Nakanishi M, Sawaguchi A, Nagai R, Takahashi K, Yamanaka S, Nakauchi H, Eto K：Transient activation of c-MYC expression is critifal for efficient platelet generation from human induced pluripotent stem cells. J Exp Med **207**(13)：2817-2830, 2010.

Cell Metabolism
Short Article

Adipose Natural Regulatory B Cells Negatively Control Adipose Tissue Inflammation

Satoshi Nishimura,[1,2,*] Ichiro Manabe,[1,*] Satoshi Takaki,[6] Mika Nagasaki,[1,3] Makoto Otsu,[7] Hiroshi Yamashita,[1] Junichi Sugita,[1] Kotaro Yoshimura,[4] Koji Eto,[8] Issei Komuro,[1] Takashi Kadowaki,[2,5] and Ryozo Nagai[9]
[1]Department of Cardiovascular Medicine
[2]Translational Systems Biology and Medicine Initiative
[3]Computational Diagnostic Radiology and Preventive Medicine
[4]Department of Plastic Surgery
[5]Department of Metabolic Diseases
Graduate School of Medicine, The University of Tokyo, Tokyo 113-8655, Japan
[6]Research Institute, National Center for Global Health and Medicine, Tokyo 162-8655, Japan
[7]Division of Stem Cell Therapy and Stem Cell Bank, Center for Stem Cell Biology and Regenerative Medicine, Institute of Medical Science, The University of Tokyo, Tokyo 108-0071, Japan
[8]Center for iPS Cell Research and Application, Kyoto University, Kyoto 606-8507, Japan
[9]Jichi Medical University, Tochigi 329-0498, Japan
*Correspondence: snishi-tky@umin.ac.jp (S.N.), manabe-tky@umin.ac.jp (I.M.)
http://dx.doi.org/10.1016/j.cmet.2013.09.017

SUMMARY

Distinct B cell populations, designated regulatory B (B_{reg}) cells, are known to restrain immune responses associated with autoimmune diseases. Additionally, obesity is known to induce local inflammation within adipose tissue that contributes to systemic metabolic abnormalities, but the underlying mechanisms that modulate adipose inflammation remain poorly understood. We identified B_{reg} cells that produce interleukin-10 constitutively within adipose tissue. B cell-specific *Il10* deletion enhanced adipose inflammation and insulin resistance in diet-induced obese mice, whereas adoptive transfer of adipose tissue B_{reg} cells ameliorated those effects. Adipose environmental factors, including CXCL12 and free fatty acids, support B_{reg} cell function, and B_{reg} cell fraction and function were reduced in adipose tissue from obese mice and humans. Our findings indicate that adipose tissue B_{reg} cells are a naturally occurring regulatory B cell subset that maintains homeostasis within adipose tissue and that B_{reg} cell dysfunction contributes pivotally to the progression of adipose tissue inflammation in obesity.

INTRODUCTION

Recent findings have shown that in addition to their capacity to produce antibodies, distinct B cell subsets, the regulatory B (B_{reg}) cells, can restrain the excessive and pathological inflammatory responses that occur during autoimmune diseases (Lemoine et al., 2009). This property of B_{reg} cells is mainly attributable to their secretion of interleukin-10 (IL-10) and/or transforming growth factor beta (TGF-β), which inhibit proinflammatory cellular processes. Several phenotypically distinct subsets of B cells, including splenic B-1a, marginal zone (MZ) B and transitional-2 (T2) MZ precursor B cells, as well as peritoneal B-1 cells, are capable of producing IL-10 upon stimulation and of negatively regulating inflammatory processes (DiLillo et al., 2010; Vitale et al., 2010). B10 cells are one of the best-characterized regulatory B cells. They are a rare subset in lymphoid tissue and bone marrow (BM), and suppress inflammatory responses in an antigen-dependent manner via IL-10 (DiLillo et al., 2010). However, only 1%–2% of splenic B cells are capable of producing IL-10 upon stimulation (IL-10 competent), and they do not constitutively produce IL-10.

Recent studies have shown that obesity induces chronic inflammation within adipose tissue, which in turn leads to metabolic abnormalities and inflammation in distant tissues. Macrophages and T cells play crucial roles in adipose inflammation (Donath and Shoelson, 2011). In lean healthy adipose tissue, inflammatory processes appear to be restricted. However, feeding a high-fat diet (HFD) to mice quickly activates $CD8^+$ T cells, which then promote macrophage accumulation and their M1 activation, thereby triggering an inflammatory cascade within visceral adipose tissue (Nishimura et al., 2009). By contrast, $CD4^+$ T_H2 and regulatory T (T_{reg}) cells, as well as resident M2 macrophages, have been shown to suppress inflammation within adipose tissue. Accordingly, it appears that the balance among immune cells is important for the maintenance of homeostasis and control of inflammatory processes within adipose tissue (Lumeng et al., 2009). However, the mechanisms by which the immune cell network controls adipose tissue inflammation are poorly understood. Recently, Winer et al. (2011) reported that adipose B cells secrete autoreactive immunoglobulin G (IgG), which contributes to adipose inflammation. However, it remains unknown whether there are B_{reg} cells present within adipose tissue, or other metabolic organs, and whether they have a regulatory function there. Herein, we describe a subset of B_{reg} cells that are abundant within adipose tissue and constitutively produce IL-10, with which they restrain adipose tissue inflammation and maintain metabolic homeostasis.

Cell Metabolism *18*, 759–766, November 5, 2013 ©2013 Elsevier Inc.

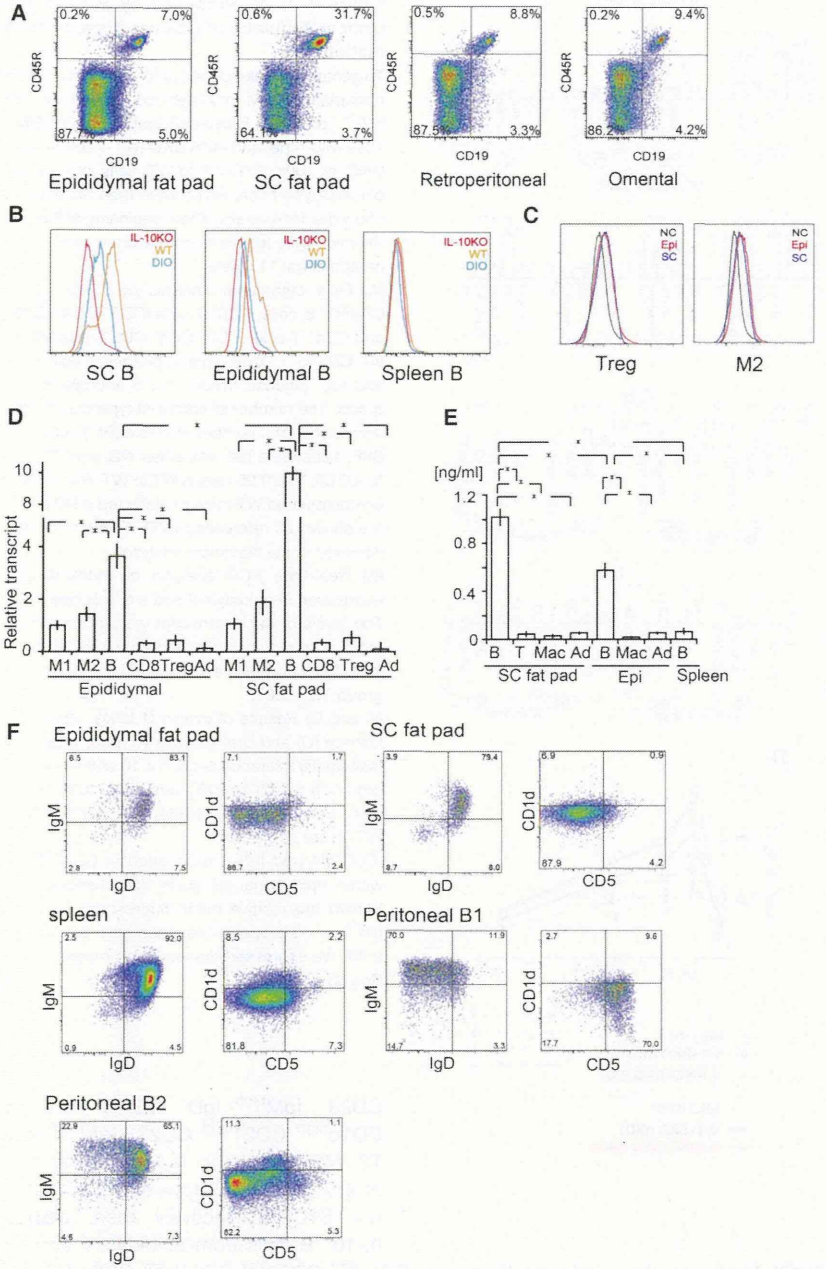

Figure 1. B Cells Constitutively Expressing IL-10 Are Abundant in Adipose Tissue

(A) Flow cytometric analysis of $CD19^+$ $CD45R^+$ B cells in the SV fraction (SVF) from epididymal, inguinal s.c. (SC), retroperitoneal, and omental fat pads from 20-week-old lean wild-type mice fed a normal chow diet (ND). Flow cytometric plots are representative of at least three independent experiments throughout this paper.

(B) Intracellular IL-10 levels in $CD19^+$ $CD22^+$ $CD45R^+$ B cells from adipose tissue and spleen from 25-week-old wild-type (WT), diet-induced obese (DIO), and *Il10*$^{-/-}$ (IL-10KO) mice. *Il10* knockout (IL-10KO) mice were used as a negative control. Note that isolated B cells were unstimulated and directly used to analyze IL-10.

(C) Intracellular IL-10 levels in $CD4^+$ $Foxp3^+$ T_{reg} cells and $F4/80^+$ $CD11c^-$ $CD206^+$ M2 macrophages from epididymal (red line) and inguinal s.c. (blue line) adipose tissue from 20-week-old lean mice. Black lines indicate the isotype-matched negative control (NC).

(D) Levels of *Il10* expression in the indicated cell types in epididymal and s.c. fat from lean control mice. Shown are levels in M1 ($F4/80^+$ $CD11c^+$ $CD206^-$) and M2 ($F4/80^+$ $CD11c^-$ $CD206^+$) macrophages, B cells ($CD19^+$ $CD22^+$ $CD45R^+$), $CD3^-$ $CD8^+$ $CD4^-$ T cells, $CD4^+$ $CD25^+$ $Foxp3^+$ T_{reg} cells, and adipocytes (Ad). n = 8 preparations, each from 5 mice. $^*p < 0.05$.

(E) B cells, $F4/80^+$ $CD11b^+$ macrophages (Mac), and adipocytes (Ad) from epididymal and inguinal s.c. adipose tissue and B cells from spleen were isolated from 20-week-old lean mice and cultured for 48 hr at a density of 5×10^4 cells/ml in Dulbecco's modified Eagle's medium (DMEM) supplemented with 10% fetal bovine serum (FBS) without LPS stimulation. IL-10 levels in the culture media were then analyzed using a multianalyte profiling system. n = 8 preparations, each from 5 mice.

(F) Flow cytometric analysis of IgM, IgD, CD1d, and CD5 expression on $CD19^+$ $CD22^+$ $CD45R^+$ B cells from adipose tissue, spleen, and peritoneum from 20-week-old ND mice. B-1 ($CD19^+$ $CD22^+$ $CD45R^{low}$) and B-2 ($CD19^+$ $CD22^+$ $CD45R^{high}$) cells were identified among the peritoneal cells. n = 5 for each medium.

We expressed the results as means ± SEM. See also Figure S1.

RESULTS AND DISCUSSION

Using flow cytometric analyses, we found that in lean C57BL/6 mice, approximately 30% of stromal vascular (SV) cells in the inguinal subcutaneous (s.c.) adipose tissue and 7%–10% of SV cells in the epididymal, retroperitoneal, and omental visceral adipose tissue are $CD19^+$ $CD22^+$ $CD45R^+$ mature B cells (Figures 1A and S1A, available online). Notably, the majority of freshly isolated, unstimulated adipose B cells contained high levels of IL-10 in their cytoplasm (Figures 1B and S1B), and the IL-10 levels were higher in s.c. than in epididymal B cells. By contrast, splenic B cells did not express IL-10 under basal conditions (Yanaba et al., 2008), nor did B cells from bone marrow (BM), peripheral blood, liver, or skeletal muscle (Figure 1B and data not shown). It was previously reported that M2 macrophages and T_{reg} cells produce IL-10. However, the levels of *Il10* mRNA expression and of intracellular IL-10 were clearly much lower in those cell types than in B cells in both s.c. and epididymal adipose tissue (Figures 1C and 1D). Moreover, when cultured, adipose B cells secreted IL-10 in the absence of lipopolysaccharide (LPS) stimulation (Figure 1E). This is in contrast to previously identified B cells, which expressed IL-10

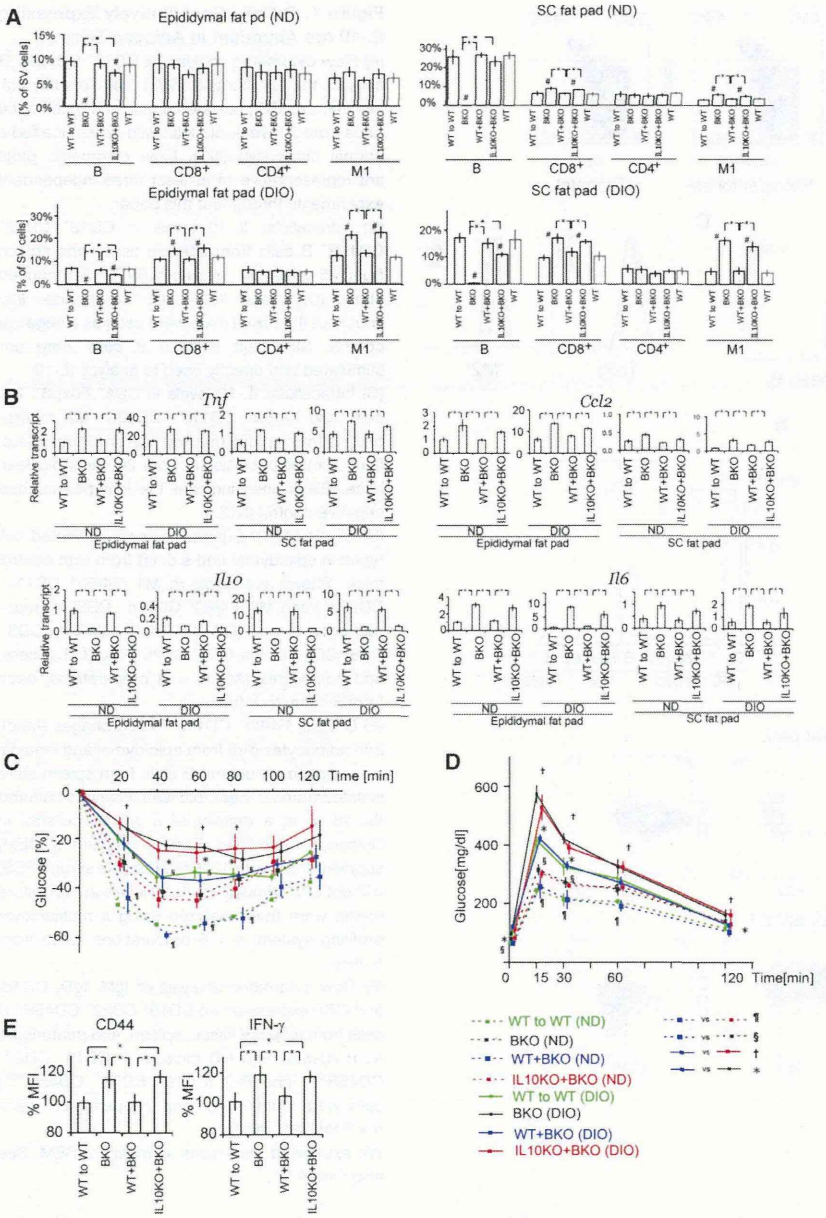

Figure 2. IL-10 Produced by B Cells Is a Critical Regulator of Adipose Tissue Inflammation

To generate B cell-specific, *Il10*-deficient mice, we transplanted BM mixtures composed of 10% *Il10*$^{-/-}$ and 90% B cell-deficient (IL10KO + BKO); 10% wild-type; and 90% BKO (WT + BKO), 100% BKO, or 100% WT (WT to WT) cells into 4-week-old wild-type mice, which were then fed a normal chow diet for 4 weeks. Then, beginning at 8 weeks, the mice were fed either normal chow or a HFD for an additional 11 weeks.

(A) Flow cytometric analysis of CD19$^+$ CD22$^+$ CD45R$^+$ B cells, CD8$^+$ T cells (CD3$^+$ CD4$^-$ CD8$^+$), and CD4$^+$ T cells (CD3$^+$ CD4$^+$ CD8$^-$) and M1 (F4/80$^+$ CD11c$^+$ CD206$^-$) macrophages in epididymal and s.c. adipose tissue. n = 5 animals in each group. The number of each cell type was normalized to the total number of viable (PI$^-$) cells in the SVF. Mice were fed with either ND or HFD (DIO). $^*p < 0.05$. $^\#p < 0.05$ versus WT to WT. Results from unmanipulated WT mice similarly fed a ND or HFD are shown as references (WT). These mice were not used in the statistical analyses.

(B) Real-time PCR analysis of cytokine gene expression in epididymal and s.c. adipose tissue. The levels of each transcript were normalized to those in epididymal adipose tissue from WT to WT mice fed a normal diet (ND). n = 8 animals in each group. $^*p < 0.05$.

(C and D) Results of insulin (1 U/kg, after 3.5 hr fasting) (C) and oral glucose (1 g/kg, after 16 hr fasting) (D) tolerance tests. n = 10 animals in each group. $^*p < 0.05$ for BKO versus WT to WT on the same diet, $^\#p < 0.05$ IL10KO + BKO versus WT to WT on the same diet.

(E) CD44 and IFN-γ production in CD8$^+$ T cells within epididymal fat pads the chimeric mice. Shown are relative mean fluorescent intensities (MFI). n = 8 preparations, each from 5 mice. $^*p < 0.05$. We expressed the results as means ± SEM. See also Figure S2.

only upon activation by LPS (DiLillo et al., 2010). Moreover, the level of IL-10 secretion from adipose tissue B cells was higher than from other cell types, including macrophages, T cells, and adipocytes (Figure 1E). Taken together, these results indicate that B cells are the major cell type expressing IL-10 in adipose tissue.

Splenic B10 cells are known to be CD1d^{high} CD5$^+$, but adipose IL-10$^+$ B cells were CD1d^{low} CD5$^{-/low}$ (Figure 1F). The surface phenotypes of adipose IL-10$^+$ B cells also differed from those of splenic and peritoneal B-1a cells, due to the low levels of CD5 and CD23 expression (Figures 1F and S1C). Likewise, the surface characteristics of adipose IL-10$^+$ B cells differed from other regulatory B cell subsets, including CD1d^{high} CD21^{high} CD23$^-$ IgM^{high} IgD$^-$ MZ B cells and CD1d^{high} CD21^{high} CD23$^+$ IgM^{high} IgD$^-$ T2 MZ precursor B cells (Mizoguchi et al., 2002; Srivastava et al., 2005)(Figure S1C). Collectively then, adipose IL-10$^+$ B cells from epididymal and s.c. adipose tissue are CD1d^{low} CD5$^{-/low}$ CD11b^{low} CD21/CD35^{low} CD23$^{-/low}$ CD25$^+$ CD69$^+$ CD72^{high} CD185$^-$ CD196$^+$ IgM$^+$ IgD$^+$, which is distinct from any other known IL-10-producing B cells.

We next hypothesized that adipose tissue IL-10$^+$ B cells negatively regulate the adipose tissue inflammation via IL-10 production. To test that hypothesis, we generated BM chimeric mice in which *Il10* was selectively deleted from B cells (Figures 2 and S2). Mixtures of 10% *Il10*$^{-/-}$ BM and 90% B cell-deficient BM (IL10KO + BKO), 10% wild-type (WT) and 90% BKO BM (WT + BKO), or 100% WT BM (WT to WT) and BKO BM (BKO) were transplanted into WT mice. Chimerism analyses showed that while the majority (approximately 90%) of T_{reg} cells and macrophages were derived from BKO BM, all B cells were derived

from IL10KO BM in IL10KO + BKO mice or WT BM in WT + BKO mice (Figure S2A). IL-10 production was not observed in B cells from IL10KO + BKO chimeric mice (Figure S2B). All the mice were then fed either a HFD or normal diet. There were no differences in body weight gains or fat pad weights among the three types of chimeric mice (Figures S2C and S2D). B cell-specific *Il10* deletion (IL10 + BKO) increased the $CD8^+$ T cell and M1 macrophage fractions in s.c. and epididymal adipose tissues from diet-induced obese (DIO) mice and in s.c. adipose tissue from lean mice (Figures 2A and S2E). In addition, levels of *Tnf*, *Ccl2*, and *Il6* expression were significantly higher in adipose tissue from IL10KO + BKO mice than in the control WT to WT mice, while IL-10 levels were much reduced, as expected (Figure 2B). These results clearly demonstrate that IL-10 produced by B cells within adipose tissue is crucial for suppression of inflammatory activation and maintenance of tissue homeostasis. As compared to the control WT to WT chimeric mice, B cell-specific *Il10*-deficient (IL10 + BKO) and B cell-deficient (BKO) chimeric mice fed a normal diet showed modest insulin resistance and glucose intolerance, and those metabolic abnormalities were aggravated by a HFD (Figures 2C and 2D). Thus, production of IL-10 by B cells appears to be important for suppressing insulin resistance, even under physiological conditions. The observation that $IL\text{-}10^+$ B cells negatively regulate inflammation and maintain homeostasis within adipose tissue indicates that the $IL\text{-}10^+$ B cells function as regulatory B cells.

$CD8^+$ T cell activation is one of the earliest events in the inflammatory processes seen during the development of obesity and is followed by M1 macrophage activation (Nishimura et al., 2009). We therefore hypothesized that B_{reg} cells may continuously suppress activation of $CD8^+$ T cells. Supporting our hypothesis was the observation that B cell-specific *Il10* deletion increased levels of CD44 and interferon gamma (IFN-γ) expression in $CD8^+$ T cells in epididymal and s.c. fat pads (Figures 2E and S2F).

To further test whether adipose B_{reg} cells are capable of inhibiting $CD8^+$ T cells locally within adipose tissue, we transplanted adipose B cells isolated from the s.c. fat pads of lean wild-type mice or splenic B cells into s.c. inguinal fat pads of obese BKO mice. The transplantation of adipose B cells reduced the levels of CD44 and IFN-γ expression in $CD8^+$ T cells, as well as levels of tumor necrosis factor alpha (TNF-α) in macrophages in the ipsilateral fat pads (Figures 3A and 3B), but this effect was not observed after splenic B cell transplantation. In addition, IFN-γ secretion from $CD8^+$ T cells was suppressed by the adipose B cell transplantation (Figure S3A). Importantly, adipose B cell transplantation did not affect $CD8^+$ T cell activation in the contralateral inguinal fat pads. Moreover, transplanting $Il10^{-/-}$ adipose tissue B cells or wild-type splenic B cells failed to inhibit $CD8^+$ T cell activation (Figures 3A and S3A).

We then tested whether B_{reg} cells might directly suppress $CD8^+$ T cells. Coculturing $CD8^+$ T cells isolated from obese s.c. adipose tissue with adipose B cells isolated from lean s.c. and epididymal adipose tissue suppressed levels of CD44 and IFN-γ expression in $CD8^+$ T cells, and this suppressive effect was eliminated by anti-iL-10 neutralizing antibody (Figure 3C). Similarly, s.c. adipose B cells suppressed IFN-γ secretion from $CD8^+$ T cells in an IL-10-dependent manner (Figure S3B). In line with those results, IL-10 suppressed expression of CD44 and IFN-γ and secretion of IFN-γ in cultured adipose $CD8^+$ T cells (Figures S3C and S3D). These findings support the notion that adipose B_{reg} cells locally suppress activation of $CD8^+$ T cells via IL-10 and that adipose B_{reg} cells play a pivotal role in the maintenance of adipose homeostasis by restraining $CD8^+$ T cells.

To further assess the functional role of B_{reg} cells in suppressing adipose tissue inflammation and in systemic metabolism, we adoptively transferred B cells to DIO mice. The initial experiments showed that adoptively transferred adipose tissue B cells efficiently accumulated in the adipose tissue, whereas B cells from the spleen and peritoneal cavity did not (Figure S3E). Thus, systemic injection could be used to transfer adipose B cells to fat depots, indicating that a mechanism exists to recruit adipose B cells to fat depots. We then transferred 5×10^5 adipose B cells to DIO mice 3 times each week for 2 weeks. Adoptive transfer of s.c. adipose tissue B cells from lean wild-type mice reduced CD44 and IFN-γ expression in $CD8^+$ T cells in both epididymal and s.c. adipose tissue (Figure 3D) and improved insulin sensitivity (Figure 3E). Notably, adoptive transfer of s.c. adipose B cells also suppressed inflammatory cytokine expression (*Tnf* and *Ccl2*) in both s.c. and epididymal fat pads (Figure 3F). Those effects were diminished when adipose B cells from DIO mice were transferred (Figures 3D–3F). In addition, s.c. adipose tissue B cells from IL-10 KO mice did not induce those effects (Figures 3D–3F). These results further support the notion that adipose B_{reg} cells negatively regulate inflammation in obese adipose tissue at least in part via IL-10 production. The results also highlight the functional difference between adipose tissue B_{reg} cells and splenic B cells.

In contrast to adipose B_{reg} cells, other regulatory B cells do not constitutively express IL-10 under physiological conditions. We therefore hypothesized that the adipose microenvironment supports the unique characteristics of adipose B_{reg} cells. Consistent with that idea, coculturing B cells with s.c. adipose tissue increased B cell production and secretion of IL-10 (Figures 4A and S4A). Coculture with fat pad also improved the survival rate among adipose B cells (Figure S4B). These results suggest the presence in adipose tissue of humoral factors that support B_{reg} cell IL-10 production and survival. Several signals have been shown to prime B_{reg} function and IL-10 secretion, including signaling in the Toll-like receptor 4 (TLR4) pathways (Yanaba et al., 2008). We therefore first tested the effects of LPS and found that LPS increased intracellular IL-10 and its secretion in both s.c. and epididymal adipose B cells (Figures 4B and S4C). On the other hand, even when treated with LPS, the amount of IL-10 secreted from splenic B cells was much smaller than that secreted from unstimulated adipose B cells. LPS also increased the viability of all B cell preparations (Figure S4D). As would be expected from these findings, pretreating s.c. and epididymal adipose B cells with LPS enhanced their suppressive effect on $CD8^+$ T cells (Figure S4E).

Previous studies have shown that saturated free fatty acids (FFAs), which are released from adipocytes through lipolysis of stored triglycerides, can activate TLR4 signaling (Eguchi et al., 2012). We therefore tested whether saturated FFAs directly affect adipose B cells and found that palmitate improved survival among cultured adipose B cells, but not splenic B cells, and induced IL-10 production in adipose B cells (Figures 4C and S4F). This suggests that the local factors within adipose tissue

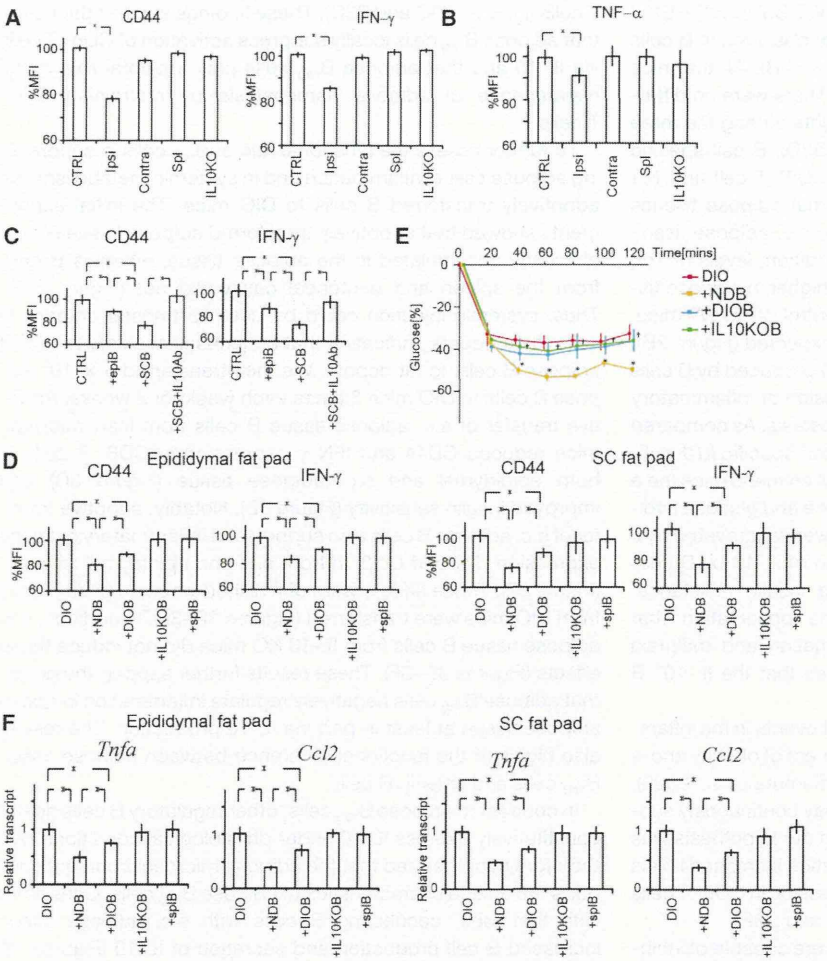

Figure 3. Adoptively Transferred Adipose B Cells Suppress Adipose Inflammation in DIO Mice

(A and B) B cells were obtained from inguinal adipose tissue and spleen from 20-week-old lean wild-type and IL-10 knockout mice. Isolated cells (5×10^5 per mouse) were injected locally into inguinal fat pads of 25-week-old obese BKO mice, and 2 days later we assessed $CD8^+$ T cell (A) and macrophage (B) activation in the treated ipsilateral (Ipsi) and contralateral (Contra) fat pads transplanted with wild-type adipose B cells and ipsilateral fat pads transplanted with splenic B cells (Spl) and adipose B cells from IL-10 KO mice (IL10KO). Subcutaneous adipose tissue of untreated age-matched DIO mice was used as a control (CTRL). Shown are relative MFIs. n = 5 preparations, each from 5 mice. *$p < 0.05$.

(C) $CD8^+$ T cells from s.c. fat pads collected from obese mice were cocultured with $CD19^+$ $CD45R^+$ B cells from s.c. (+SCB) and epididymal (+epiB) fat pads collected from lean mice or s.c. B cells plus anti-iL-10 neutralizing antibody (10 μg/ml) (+SCB + IL10Ab). The phenotypes of the $CD8^+$ T cells were analyzed after 48 hr. $CD8^+$ T cells cultured alone served as a control (CTRL). n = 5 preparations, each from 5 mice.

(D–F) B cells were isolated from s.c. fat pad from 25-week-old lean (+ND B) and obese (+DIO B) WT mice and lean IL-10 KO mice (+IL10KO B) as well as from splenic B cells from WT mice (+spl B). Thereafter, 24-week-old WT DIO mice were intravenously administered 5×10^5 cells per mouse three times each week. After administration for 2 weeks, insulin tolerance test (ITT) experiments and flow cytometric analysis of s.c. fat pads were performed. We compared adoptively transferred mice with vehicle-treated WT DIO mice serving as a control (DIO). In (D), CD44 and IFN-γ expression in $CD8^+$ T cells within epididymal and s.c. adipose tissues was analyzed. n = 8 mice. In (E), results of ITTs (1 U/kg, after 3.5 hr fasting) are shown. n = 10 animals in each group. *$p < 0.05$ for DIO versus +ND B; †$p < 0.05$ for +ND B cell versus +DIO B cell. (F) shows real-time PCR analysis of cytokine gene expression in epididymal and s.c. adipose tissue. The levels of each transcript were normalized to those in adipose tissue from control DIO mice. n = 8 animals in each group; *$p < 0.05$. We expressed the results as means ± SEM. See also Figure S3.

that activate TLR4 signaling, including FFAs, contribute to the unique functions of adipose B_{reg} cells.

To further identify the microenvironmental factors supporting adipose B_{reg} cells, we used PCR arrays to systematically analyze the gene expression of cytokine and chemokine receptors. This analysis revealed that two receptor genes, *Il10ra* and *Cxcr4*, were expressed more strongly in adipose than in splenic B cells (Figure 4D). We then assessed the effects of the ligands for those receptors. We found that IL-10 itself increased levels of intracellular IL-10 and its secretion from both s.c. and epididymal adipose B cells, but not splenic B cells (Figures 4B and S4C). IL-10 also improved the viability of adipose B cells, but not splenic B cells (Figure S4D). Moreover, addition of an anti-IL-10 neutralizing antibody partially inhibited the prosurvival effect of adipose tissue on adipose B cell viability (Figure S4B), and pretreating adipose B cells with IL-10 augmented their suppressive effects on $CD8^+$ T cells (Figure S4E). These results show that IL-10 enhances adipose B cell survival and function in vitro.

Inhibition of IL-10 signaling through systemic administration of an anti-IL-10 neutralizing antibody modestly, but significantly, reduced the B cell fraction in adipose tissue, but not in bone marrow, spleen, liver, or skeletal muscle (Figures S4G and S4H). As expected, IL-10 neutralization also increased CD44 and IFN-γ expression in adipose $CD8^+$ T cells (Figure S4I). Genetic *Il10* deletion reduced B cell numbers in fat pads, but not in bone marrow, spleen, liver, or skeletal muscle (Figure S4J). These results suggest that IL-10 is one of the environmental factors present in adipose tissue, though the presence of B cells in the adipose tissue of IL-10 knockout mice suggests that other factors are also involved.

We next analyzed the C-X-C chemokine receptor type 4 (CXCR4) ligand CXCL12. *Cxcl12* was expressed in SV cells within all the adipose tissues analyzed (i.e., inguinal, epididymal, omental, and retroperitoneal fat), and its expression levels were higher in adipose SV cells than in spleen (Figure 4E and data not shown), suggesting that CXCL12 might contribute to B cell accumulation in adipose tissue. To test this idea, we locally injected

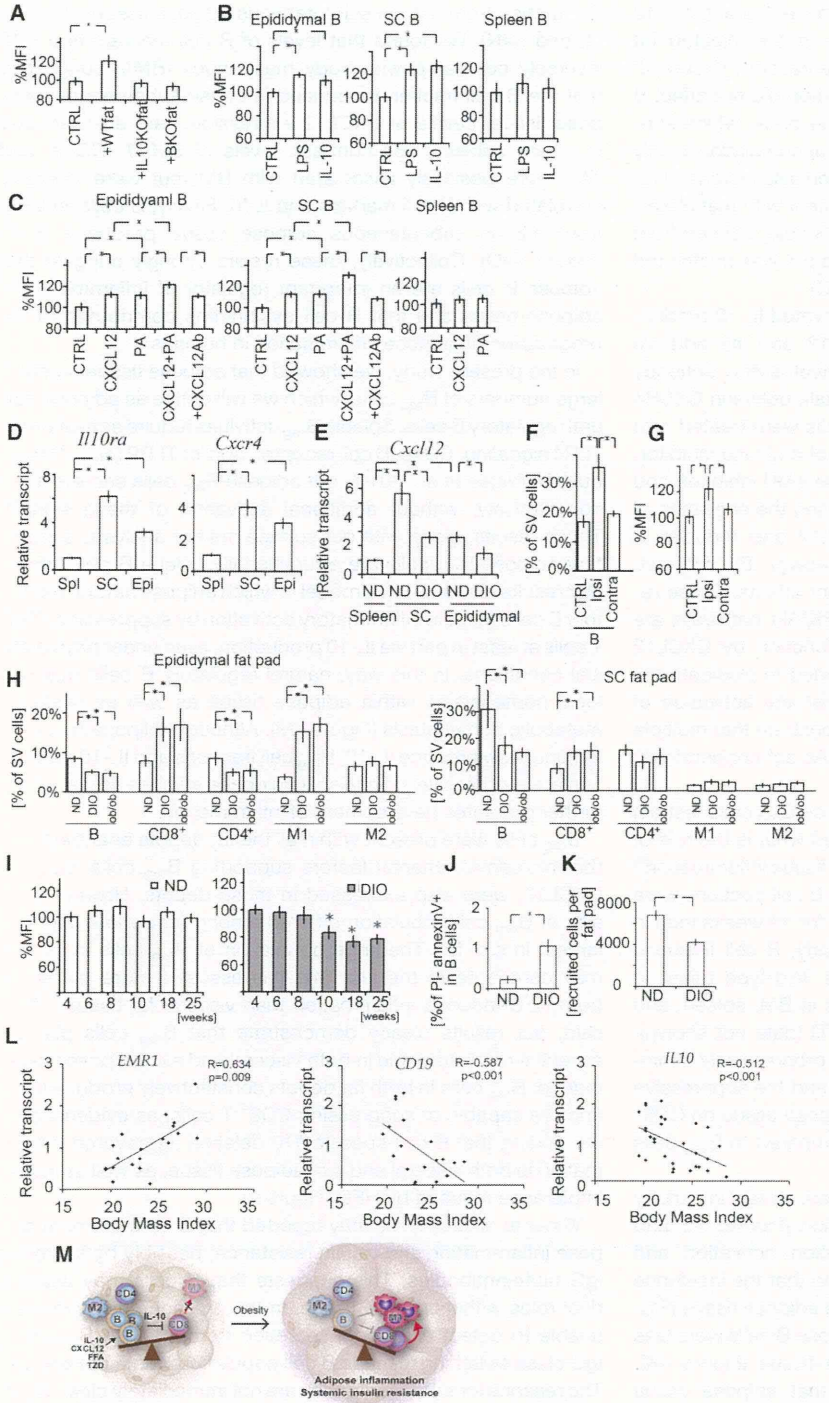

Figure 4. Environmental Factors within Adipose Tissue Support B_{reg} Cell Survival and Function

(A) B cells were incubated for 48 hr in the presence of pieces of s.c. adipose tissue from WT (+WTfat), IL-10 knockout (+IL10KOfat), or BKO (+BKOfat), after which their IL-10 production was analyzed. n = 5 experiments in each group.

(B) Intracellular production of IL-10 in B cells after incubation for 48 hr with LPS (1 μg/ml) or recombinant IL-10 (10 ng/ml). n = 5 preparations, each from 5 mice.

(C) Cultured B cells isolated from spleen and epididymal and s.c. fat pads from 20-week-old lean mice were treated for 48 hr with vehicle (CTRL), palmitate (PA; 100 μM), or recombinant CXCL12 (10 ng/ml), after which intracellular IL-10 production was analyzed. Neutralizing anti-CXCL12 antibody (10 μg/ml) was also added to some cells treated with palmitate and CXCL12 (+CXCL12Ab). n = 5 experiments in each group.

(D) Expression of *Il10ra* and *Cxcr4* in B cells in spleen and epididymal or s.c. fat pad from lean mice. n = 5 animals in each group.

(E) Expression of *Cxcl12* (SDF-1, CXCR4 ligand) in the SV fractions of s.c. and epididymal adipose tissues, and spleen from 25-week-old lean and DIO mice. n = 5 animals.

(F and G) Mice were fed a HFD for 21 weeks, beginning when they were 4 weeks old, and were administered CXCL12 (0.5 μg per g body weight) into an inguinal fat pad daily for 2 weeks. Age-matched obese mice served as controls (CTRL). In (F), the relative B cell fractions in the treated ipsilateral (Ipsi) or contralateral (Contra) fat pads are shown. In (G), intracellular IL-10 in B cells in s.c. fat pads is shown. n = 5 experiments in each group; $^*p < 0.05$.

(H) Flow cytometric analysis of immune cells in epididymal and s.c. fat pads from lean mice fed a normal chow diet (ND); diet-induced-obese (DIO) mice fed a HFD for 16 weeks, beginning when they were 4 weeks old; and ob/ob mice fed a ND. All mice were analyzed when they were 20 weeks old. The number of each cell type was normalized to the total number of viable (PI^-) cells in the SVF, and fractions among viable cells are shown. The total number of each cell type per fat depot is shown in Figure S4L. n = 5 animals in each group. $^*p < 0.05$.

(I) Intracellular IL-10 in B cells isolated from mouse s.c. adipose tissue at the indicated ages. The DIO mice were fed a HFD, beginning when the mice were 4 weeks old. $^*p < 0.05$ versus 4 weeks old.

(J) Fractions of early apoptotic (Annexin V^+ PI^-) cells among B cells in s.c. adipose tissue from 25-week-old DIO mice. n = 5 animals.

(K) B cells (2×10^5 cells per g body weight) obtained from inguinal adipose tissue were adoptively transferred into 25-week-old lean and DIO mice. Shown is the total number of transferred B cells detected within each s.c. fat pad. n = 5 animals in each group.

(L) Levels of gene expression in the SV fractions of s.c. fat pads obtained at surgery from human subjects and body mass index values were analyzed. R values were calculated using Pearson's correlation coefficient test. Expression levels were normalized to the average of all subjects. n = 20 subjects.

(M) Schematic model of B cell function in adipose homeostasis and inflammation. We expressed the results as means ± SEM. See also Figure S4.

CXCL12 into s.c. inguinal fat pads of DIO mice. Local CXCL12 selectively increased the B cell fractions in the injected fat pads without affecting T cell or macrophage fractions (Figure 4F and data not shown). By contrast, the injection did not affect B cell fractions in the contralateral inguinal fat pads, which supports the notion that CXCL12 affects B cell accumulation locally within the injected fat pads. CXCL12 injection also increased IL-10 production in B cells (Figure 4G). Consistent with that observation, IL-10 production was enhanced in B cells isolated from adipose tissue treated with CXCL12 ex vivo but was unaffected in splenic B cells treated likewise (Figure 4C).

Notably, addition of palmitate further activated IL-10 production in adipose B cells treated with CXCL12, and this additive effect was blocked by an anti-CXCL12 neutralizing antibody (Figure 4C), suggesting that there is crosstalk between CXCR4 and TLR4 signaling. To test that idea, B cells were treated with palmitate and/or CXCL12 in the presence of a kinase inhibitor. We found that both BMS345541 (IκB kinase [IKK] inhibitor) and LY294002 (PI3K inhibitor) partially suppressed the activation of IL-10 production by palmitate and CXCL12 and reduced B cell survival (Figure S4K and data not shown). By contrast, PD98059 (MEK1 inhibitor) had no significant effects. These results suggest that both the NF-κB and PI3K/Akt pathways are important for the activation of B_{reg} cell function by CXCL12 and FFA. However, further studies are needed to elucidate the signaling crosstalk underlying the combinatorial activation of B_{reg} cells. Collectively, these findings demonstrate that multiple environmental mediators and saturated FFAs act cooperatively to support adipose B_{reg} cells.

The results so far demonstrate that adipose B_{reg} cells restrain adipose tissue inflammation. We then asked what is the role of B_{reg} cells during the progression of adipose tissue inflammation? In both s.c. and visceral adipose tissue, the B cell fractions were significantly smaller in DIO mice fed a HFD for 16 weeks than in lean controls (Figures 4H and S4L). Similarly, B cell fractions were smaller in ob/ob mice than in lean wild-type mice. In contrast to adipose tissue, B cell fractions in BM, spleen, and peripheral blood were unaffected by a HFD (data not shown). Moreover, IL-10 expression in B cells was progressively diminished in adipose tissue by DIO (Figure 4I), and the suppressive effect of B_{reg} cells isolated from obese adipose tissue on $CD8^+$ T cell activation was compromised, as compared to B_{reg} cells from lean adipose tissue (Figure 3D).

The smaller B cell fraction may be explained, at least in part, by the reduction in *Cxcl12* and *Il10* expression (Figures 4E and S4M), which could affect B cell accumulation, activation, and survival. Consistent with that idea, we found that the incidence of apoptotic B cells was increased in obese adipose tissue (Figure 4J) and that adoptively transferred adipose B cells were less efficiently accumulated in obese adipose tissue (Figure 4K). Taken together, these findings suggest that adipose tissue obesity alters environmental cues (i.e., CXCL12 and IL-10) important for B cell recruitment, survival, and activation, and the resultant B_{reg} cell dysfunction contributes to the progression of adipose tissue inflammation.

To gain insight into the clinical significance of adipose B cells in humans, we analyzed the expression levels of several cytokines (*TNF*, *CCL2*, *IL10*, *CXCL12*, and *MIF*) as well as markers of B cells (*CD19* and *CD22*) and macrophages (*EMR1*) in the SV fraction from human subcutaneous adipose tissues (Figures 4L and S4N). We found that levels of B cell markers and *IL10* inversely correlated with body mass index (BMI), suggesting that the B cell fraction is reduced in obese subcutaneous adipose tissue. Levels of *CXCL12* expression were also reduced in obese subjects. By contrast, levels of *EMR1*, *CCL2*, and *TNF* were positively associated with BMI but were inversely correlated with B cell markers and *IL10*. Finally, B cells isolated from human subcutaneous adipose tissue produced IL-10 (Figure S4O). Collectively, these results strongly suggest that adipose B cells are an important regulator of inflammation in adipose tissue and that B cell dysfunction contributes to the progression of adipose inflammation in humans.

In the present study, we showed that adipose tissue contains large numbers of B_{reg} cells, which we will define as adipose natural regulatory B cells. Splenic B_{reg} activities require activation via TLR4 signaling, CD40, B cell receptor, and/or TLR9 for IL-10 production (Vitale et al., 2010), but adipose B_{reg} cells secrete IL-10 constitutively, without additional activation of these signals. Those results, along with our surface marker analysis, suggest that adipose B_{reg} cells are a functionally unique B cell subset. Our results also support a model in which adipose natural regulatory B cells restrain inflammatory activation by suppressing $CD8^+$ T cells at least in part via IL-10 production, even under physiological conditions. In this way, natural regulatory B cells maintain local homeostasis within adipose tissue as well as systemic metabolic homeostasis (Figure 4M). Although adipose B_{reg} cells continuously produce IL-10, B_{reg} cell fractions and IL-10 production are progressively diminished in obese adipose tissue, which further promotes development of inflammation.

B_{reg} cells were present within all the fat depots analyzed, and the microenvironmental factors supporting B_{reg} cells, such as CXCL12, were also expressed in those depots. However, the size of B_{reg} cell population differed among fat depots and was largest in s.c. fat. The large population of B_{reg} cells in s.c. fat may contribute to the fact that this tissue is more protected from HFD-induced inflammation than visceral fat tissues. That said, our results clearly demonstrate that B_{reg} cells play an essential regulatory role in both visceral and s.c. adipose tissue. Indeed, B_{reg} cells in both fat depots constitutively produce IL-10 and are capable of suppressing $CD8^+$ T cells, as evidenced by our finding that B cell-specific *Il10* deletion aggravated inflammation in both visceral and s.c. adipose tissue, as well as insulin intolerance induced by HFD (Figure 2).

Winer et al. (2011) recently reported that B cells promote adipose inflammation and insulin resistance, possibly by secreting IgG (auto)antibodies. This suggests that B cells may assume dual roles within adipose tissue. In the present study, we were unable to detect either IgG secretion from adipose B cells or IgG class switching in major B cell populations (data not shown). The reasons for this discrepancy are not immediately clear. However, we found that both the number of adipose tissue B_{reg} cells and the IL-10 production were higher in adipose B cells in germ-free mice than specific pathogen-free (SPF) mice (data not shown). It is tempting to speculate that endogenous and environmental factors affect adipose B cell phenotypes.

In conclusion, we have identified adipose natural regulatory B cells, which are crucial for maintaining homeostasis within adipose tissue. Our results suggest that controlling adipose natural

regulatory B cell function could serve as the basis for novel approaches to the treatment of metabolic syndrome and other obesity-related diseases.

EXPERIMENTAL PROCEDURES

Animals

B cell-deficient mice were described previously (Kitamura et al., 1991). Full methods and any associated references are available in the Supplemental Information. All experiments were approved by the University of Tokyo Ethics Committee for Animal Experiments and strictly adhered to the guidelines for animal experiments of the University of Tokyo.

Human Subjects

After obtaining informed consent using an institutional review board-approved protocol, we acquired subcutaneous adipose tissue from healthy female donors undergoing liposuction of the abdomen or thighs.

SUPPLEMENTAL INFORMATION

Supplemental Information includes Supplemental Experimental Procedures and four figures and can be found with this article online at http://dx.doi.org/10.1016/j.cmet.2013.09.017.

ACKNOWLEDGMENTS

We are very grateful to M. Tajima, C. Yoshinaga, X. Yingda, and T. Hirabayashi for their excellent technical help. This study was supported by the Funding Program for Next Generation World-Leading Researchers (S.N.); the Funding Program for World-Leading Innovative R&D on Science and Technology (FIRST Program) (R.N.); JSPS KAKENHI grants 20390220 and 23390203 (I.M.); Grants-in-Aid for Scientific Research on Innovative Areas "Fluorescence Live imaging" (22113008) (S.N.) and "Homeostatic Inflammation" (22117504 and 24117703) (I.M.); the global COE program (R.N., T.K.) from MEXT, Japan; the Translational Systems Biology and Medicine Initiative (R.N. and T.K.) from JST; and grants from the National Center for Global Health and Medicine (S.T.) and Banyu Life Science Foundation International (S.N.). The authors declare that no competing interests exist.

Received: May 15, 2013
Revised: August 1, 2013
Accepted: September 6, 2013
Published: October 24, 2013

REFERENCES

DiLillo, D.J., Matsushita, T., and Tedder, T.F. (2010). B10 cells and regulatory B cells balance immune responses during inflammation, autoimmunity, and cancer. Ann. N Y Acad. Sci. *1183*, 38–57.

Donath, M.Y., and Shoelson, S.E. (2011). Type 2 diabetes as an inflammatory disease. Nat. Rev. Immunol. *11*, 98–107.

Eguchi, K., Manabe, I., Oishi-Tanaka, Y., Ohsugi, M., Kono, N., Ogata, F., Yagi, N., Ohto, U., Kimoto, M., Miyake, K., et al. (2012). Saturated fatty acid and TLR signaling link β cell dysfunction and islet inflammation. Cell Metab. *15*, 518–533.

Kitamura, D., Roes, J., Kühn, R., and Rajewsky, K. (1991). A B cell-deficient mouse by targeted disruption of the membrane exon of the immunoglobulin mu chain gene. Nature *350*, 423–426.

Lemoine, S., Morva, A., Youinou, P., and Jamin, C. (2009). Regulatory B cells in autoimmune diseases: how do they work? Ann. N Y Acad. Sci. *1173*, 260–267.

Lumeng, C.N., Maillard, I., and Saltiel, A.R. (2009). T-ing up inflammation in fat. Nat. Med. *15*, 846–847.

Mizoguchi, A., Mizoguchi, E., Takedatsu, H., Blumberg, R.S., and Bhan, A.K. (2002). Chronic intestinal inflammatory condition generates IL-10-producing regulatory B cell subset characterized by CD1d upregulation. Immunity *16*, 219–230.

Nishimura, S., Manabe, I., Nagasaki, M., Eto, K., Yamashita, H., Ohsugi, M., Otsu, M., Hara, K., Ueki, K., Sugiura, S., et al. (2009). CD8+ effector T cells contribute to macrophage recruitment and adipose tissue inflammation in obesity. Nat. Med. *15*, 914–920.

Srivastava, B., Quinn, W.J., 3rd, Hazard, K., Erikson, J., and Allman, D. (2005). Characterization of marginal zone B cell precursors. J. Exp. Med. *202*, 1225–1234.

Vitale, G., Mion, F., and Pucillo, C. (2010). Regulatory B cells: evidence, developmental origin and population diversity. Mol. Immunol. *48*, 1–8.

Winer, D.A., Winer, S., Shen, L., Wadia, P.P., Yantha, J., Paltser, G., Tsui, H., Wu, P., Davidson, M.G., Alonso, M.N., et al. (2011). B cells promote insulin resistance through modulation of T cells and production of pathogenic IgG antibodies. Nat. Med. *17*, 610–617.

Yanaba, K., Bouaziz, J.D., Haas, K.M., Poe, J.C., Fujimoto, M., and Tedder, T.F. (2008). A regulatory B cell subset with a unique CD1dhiCD5+ phenotype controls T cell-dependent inflammatory responses. Immunity *28*, 639–650.